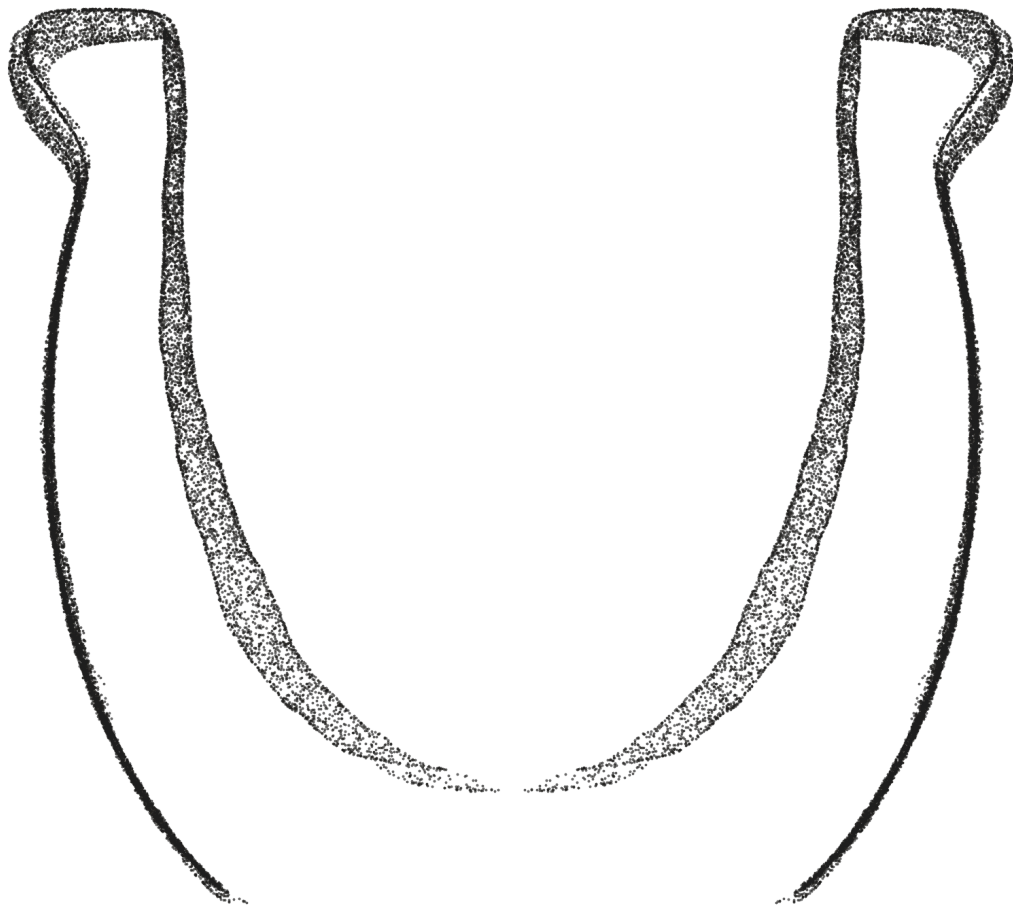


# MV006 - Globular Ovoid Jar

An Exploration of Precision



Author: Stine Gerdes, [arcsoci.org](http://arcsoci.org)

License: Creative Commons BY-NC-SA 4.0

Date: 2025-03-18

Version: 01.00



Petrie Museum, CC BY-NC-SA

**Contents**

**Artifact Information ..... 2**

**Alignment In The Cartesian Coordinate System ..... 3**

**Precision ..... 5**

Circularity ..... 5

Concentricity ..... 24

Coaxiality ..... 35

Surface Variability ..... 38

Precision Score Of The Artifact ..... 45

**Analysis Roadmap ..... 47**

**Appendix A - Comparison Of Circularity Measurements (Z-plane vs. surface-perpendicular) ..... 48**

**Appendix B - Comparison Of Concentricity Measurements (Z-plane vs. surface-perpendicular) ..... 55**

# Artifact Information

## Artifact Data

Collection	Petrie Museum of Egyptian Archaeology
Provenance <sup>1</sup>	Petrie Museum of Egyptian Archaeology (London), recovered by Flinders Petrie
Provenience <sup>2</sup>	William Matthew Flinders Petrie excavation
Attribution	Predynastic Period

## Museum information

Ref.	LDUCE-UC15724
Description	Basalt cylinder vase, tapering at base, rim damaged
URL	<a href="https://collections.ucl.ac.uk/Details/collect/24117">https://collections.ucl.ac.uk/Details/collect/24117</a>

## Maijers vessel classification<sup>3</sup>

Short classification	Globular Ovoid Jar
Long classification	The vessel is created in a closed form classified as a globular jar with a ovoid shape, a raised blunt rim.

## Physical properties

Precision score <sup>4</sup>	9
Height (approximate)	65 mm    2.56 in
Width (approximate)	70 mm    2.76 in
Material	Basalt
Mohs Hardness <sup>5</sup>	5 - 7 (Basalt)
Weight	

## Scan information

Source	Scanned by Artifact Foundation
Source file name	UC15724_base_0.09.stl
Scan method	Laser
Scanner	FreeScale Combo+
Rated scan accuracy	37 µm   1.51 thou
Scan date	2024-10-07
Scanned by	Adam Young and Károly Póka
Mesh decimation	None, raw scan file used in the analysis
Number of vertices	4 352 705
Mesh density <sup>6</sup>	35 µm   1.38 thou
Max vertex distance	132 µm   5.211 thou
Min vertex distance	0 µm   0.000 thou
Vertices per cm <sup>2</sup>	19 081 (approximated)
Vertices per in <sup>2</sup>	123 102 (approximated)

---

<sup>1</sup>The verifiable chain of custody of an artifact

<sup>2</sup>The location or site where an artifact was recovered

<sup>3</sup>Vessel artifact classification developed by W. Arnold Maijer and described in his publication Masters of Stone, ISBN 978-90-829212-0-5

<sup>4</sup>The precision score metric is described in Precision Score Of The Artifact, p. 46

<sup>5</sup>The Mohs scale is an ordinal scale, from 1 to 10, describing the materials resistance to abrasion (the ability of harder material to scratch softer material)

<sup>6</sup>Median distance between vertices

## Alignment In The Cartesian Coordinate System

For precise and valid measurements of the vessel's geometry to be possible, the points of the scanned dataset must first and foremost be placed optimally in a Cartesian coordinate system. Several alignment methods and algorithms have been tested on a number of different vessels to determine the best way to achieve optimal alignment.

Any misalignment of the artifact will increase the error of the precision measurements, due to the distortion/wobble effect caused by the misaligned object. To visualize this distortion, we can consider a representation of the three-dimensional point cloud data, folded to a two-dimensional plane. This folded representation is obtained by rotating all scanned points around an assumed center axis to  $y = 0, x > 0$ , thus resulting in a two-dimensional profile representation of all scanned vertices in the object.

Figure 1 illustrates this effect on a ideal ellipsoid. In the first image, the ellipsoid is perfectly aligned, resulting in a narrow and precise two-dimensional folded profile. As misalignments are introduced, the two-dimensional profile increases in width, visually showing the distortion, causing the error in the precision measurements to increase. While easy to understand visually, this distortion can also be objectively quantified, and as such used to compare the fitness of different assumed center axes against each other, and further to create an automated and solid process for optimal Cartesian alignment of the scan data.

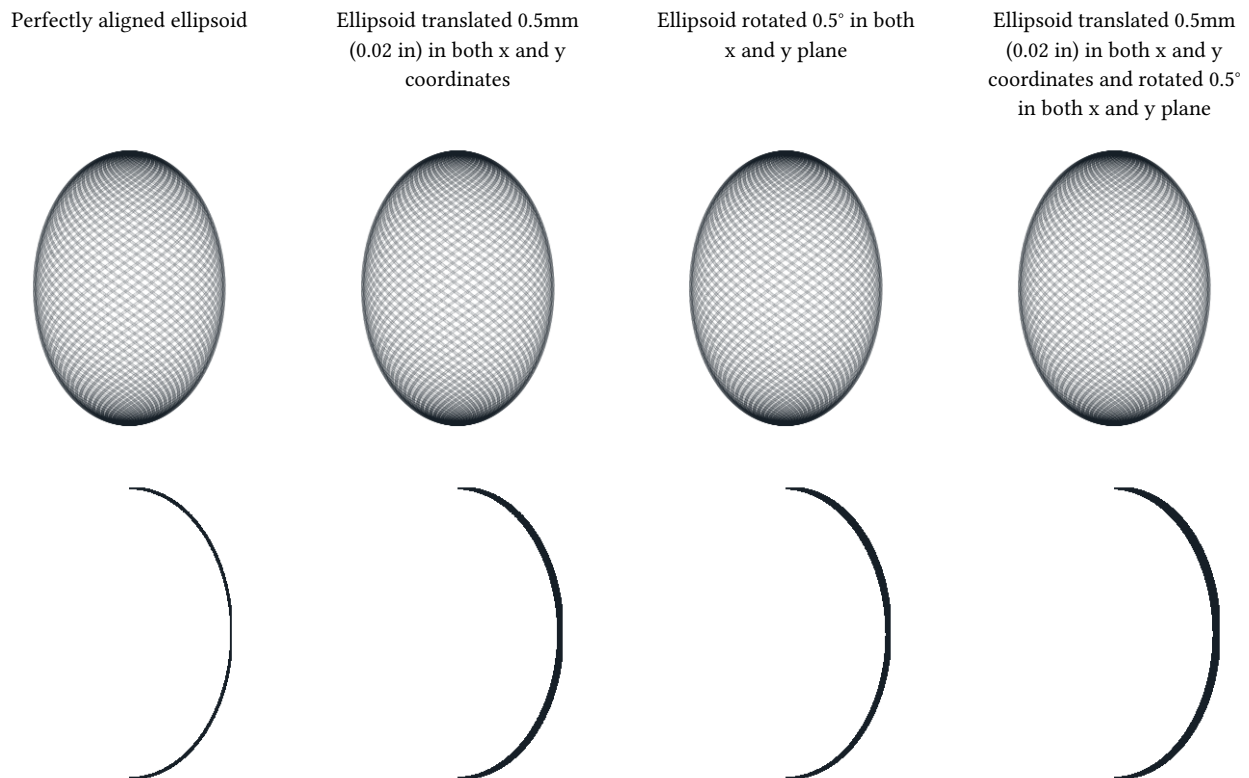


Figure 1: Distortion caused by a misalignment of the artifact

In contemporary metrology analysis of modern production objects, it is common to align the object in a Cartesian coordinate system by fitting a flat surface of the object to a reference plane in the coordinate system, cylindrical features to an ideal cylinder etc., or by using specific markers placed on the object in the design process. This methodology, however, is inadequate for the ancient objects in question. Most scanned artifacts, do not have a valid flat surface which could be aligned to a plane in the Cartesian coordinate system; most surfaces seem to be curved. Some artifacts do have a flat base, however this is often a worn area of the artifact and practical tests have shown that alignment to such surfaces will not produce optimal alignment of the scan data.

As conventional methods of alignment do not always yield good results with these types of artifacts, a more adequate method of alignment has been developed to enable precise measurements and statistical analysis of the scan data.

To find the optimal position of the vessel in the coordinate system, a range of rotation and translation tests are carried out to find the best fit of the central axis.

Based on the assumption that the analyzed object was created using a rotational process, and thus have symmetry around a central axis, the alignment of the artifact is carried out in a two-step process. An overview of this process is given below.

The artifact is placed in a Cartesian coordinate system, in an initially unaligned state. The first step in the alignment process estimates the central rotational axis of the vessel, by analyzing the coaxiality of thin cross-section slices of the vessel. The slices will be as thin as possible based on the mesh density of the scan, while still ensuring enough data points in each slice to be statistically valid.

For each slice, circular regression<sup>7</sup> (estimate of best fit circle) is used to estimate the center point of this slice. Combined over the total Z-axis range of the vessel, these center points provide us with an indicator of the incline and position of the vessel's central axis.

The next step will optimize the center axis alignment by progressively minimizing the deviation (perpendicular to the surface curvature) of the two-dimensional profile, see Figure 1. By ascertaining and comparing the resulting fit of many thousands of different potential rotations, the best fit alignment of the scan data can be estimated, and an optimal center axis (in relation to the data points) can be reconstructed. The actual three-dimensional point-cloud is then aligned to this axis, by rotating and translating the scanned data points to match the Z-axis of the Cartesian coordinate system.

---

<sup>7</sup>Circle regression algorithm used: Kenichi Kanatani, Prasanna Rangarajan, "Hyper least squares fitting of circles and ellipses" Computational Statistics & Data Analysis, Vol. 55, pages 2197-2208, (2011)

## Precision

To explore the manufacturing precision of the artifact in depth, the following analysis have been carried out:

- Circularity around the axis of symmetry is examined in detail at selected cross-sections.
- Overall circularity around the axis of symmetry is measured for the full height of the vessel (areas of the vessel with extensive damage are not taken into account for this metric).
- Concentricity of the vessel between selected cross-sections are examined in detail to determine if the existence of an axis of rotation in the manufacture of the object can be established.
- The coaxiality of the vessel is analyzed to explore the precision of the central axis of the object.
- The surface variability is analyzed and visualized on through a heatmap.

## Circularity

Circularity is the measurement of how round the surface of an object is, optionally in reference to a datum axis. The *circularity tolerance* is the radial distance of two circles, each with their centers in the datum axis, and each of them conforming, respectively, to the minimum and maximum deviations of the data-set to a true circle, see Figure 2.

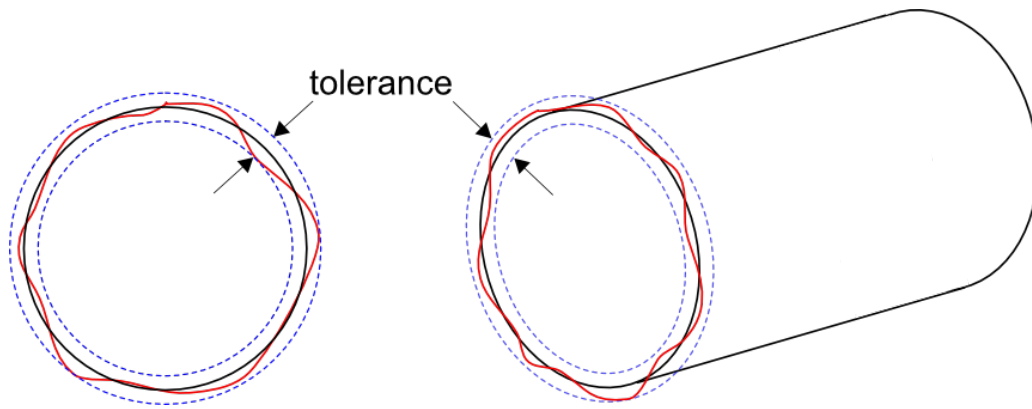


Figure 2: Circularity tolerance.

Circularity is examined at different cross-sections of the vessel, using the established Z-axis as the datum axis (axis of symmetry). The distance between the scanned points in the local datum plane is measured to determine the range between the two concentric circles encompassing the measured points, see Figure 3.

Referencing all of the individual circularity measurements to the global (reconstructed) axis of symmetry of the object, allows us to ascertain not only circularity of local features of the object, but how well circularity was *maintained* over the entire manufacturing process. This is an important distinction, which may be able to provide valuable insights into requirements of the construction methods. For reference, and seeing that the variance in local circularity also holds interest, measurements of circularity of the vessel without reference to the axis of symmetry can additionally be found in the Concentricity, p. 25.

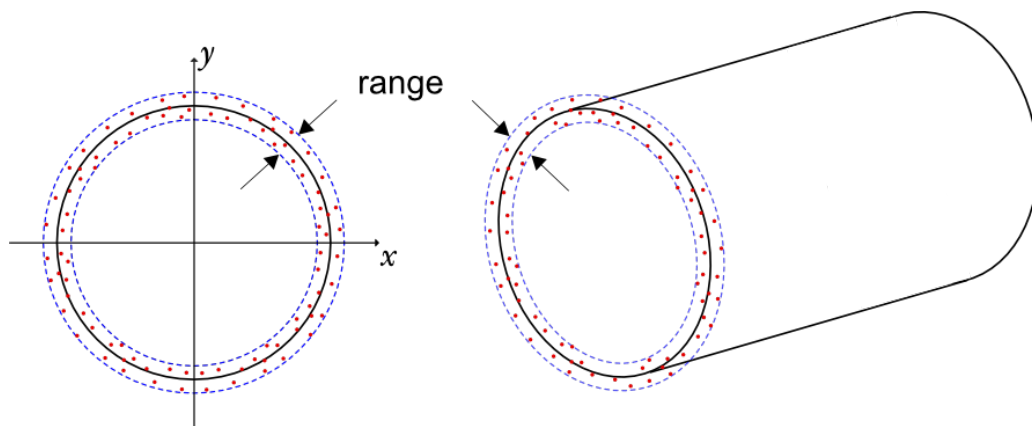


Figure 3: Circularity measurements.

If the circularity is determined from slices of the vessel exclusively in the *Z-plane* (actually measuring the cylindricity of a very thin slices of the vessel, in an attempt to approximate circularity), this would - in some areas - introduce significant distortion (increasing measurement errors) in the samples, due to the curvature of the vessel's surface.

Each sample slice of the vessel is therefore obtained perpendicular to the surface curvature, see Figure 5 to Figure 13. The measurements are taken conservatively without filtration of potential outliers.

To explore the potential distortion caused by obtaining samples in the Z-plane only, please refer to Appendix A, where measurements in the Z-plane and measurements perpendicular to surface curvature are compared side by side.

#### **Detailed circularity measurements of selected points**

Circularity measurements across a range of selected slices of the vessel (see Table 1) have been analyzed in-depth, and detailed plots of each measurement is provided. Furthermore, full circularity measurements are shown for each available scanned surface including a detailed plot to visualize the circularity of all areas of the vessel.

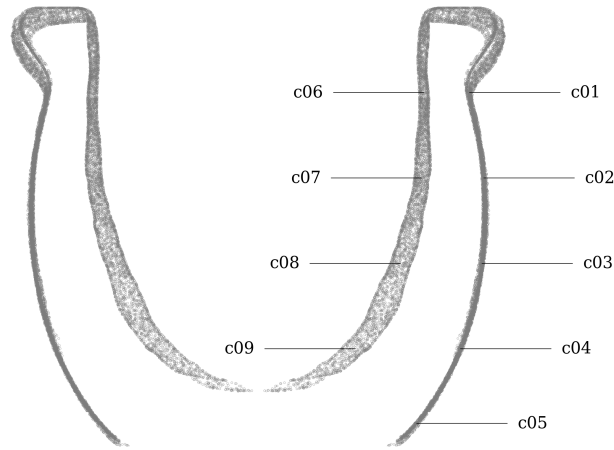


Figure 4: Circularity measurement sample location on MV006.

### Metric

Tag	Area	Measured deviation <sup>8</sup>	Residuals				Sample size	Slice		
			Range	RMSD <sup>9</sup>	MAD <sup>10</sup>	SD		Height	Z coord.	Radius <sup>11</sup>
		mm	mm	mm	mm	mm		mm	mm	mm
c01	exterior	Ø62.863±0.516	1.012	0.275	0.196	0.276	1762	0.050	52.209	31.431
c02	exterior	Ø67.109±0.436	0.812	0.167	0.117	0.167	1960	0.050	39.545	33.555
c03	exterior	Ø66.558±0.503	0.818	0.191	0.132	0.191	2010	0.050	26.881	33.279
c04	exterior	Ø60.183±0.756	1.124	0.187	0.134	0.187	1645	0.050	14.218	30.091
c05	exterior	Ø47.151±0.437	0.714	0.167	0.107	0.167	1108	0.050	3.154	23.576
c06	interior	Ø49.365±0.754	1.411	0.459	0.449	0.460	1491	0.050	52.209	24.683
c07	interior	Ø48.677±1.141	2.165	0.763	0.788	0.763	1451	0.050	39.545	24.339
c08	interior	Ø42.346±1.493	2.937	1.016	0.992	1.017	1132	0.050	26.881	21.173
c09	interior	Ø28.936±1.626	2.778	0.999	0.928	0.988	698	0.050	14.218	14.468

### Imperial

Tag	Area	Measured deviation <sup>8</sup>	Residuals				Sample size	Slice		
			Range	RMSD <sup>9</sup>	MAD <sup>10</sup>	SD		Height	Z coord.	Radius <sup>11</sup>
		in	in	in	in	in		in	in	in
c01	exterior	Ø2.4749±0.0203	0.0398	0.0108	0.0077	0.0108	1762	0.0020	2.0555	1.2375
c02	exterior	Ø2.6421±0.0172	0.0320	0.0066	0.0046	0.0066	1960	0.0020	1.5569	1.3210
c03	exterior	Ø2.6204±0.0198	0.0322	0.0075	0.0052	0.0075	2010	0.0020	1.0583	1.3102
c04	exterior	Ø2.3694±0.0298	0.0442	0.0073	0.0053	0.0073	1645	0.0020	0.5598	1.1847
c05	exterior	Ø1.8564±0.0172	0.0281	0.0066	0.0042	0.0066	1108	0.0020	0.1242	0.9282
c06	interior	Ø1.9435±0.0297	0.0555	0.0181	0.0177	0.0181	1491	0.0020	2.0555	0.9718
c07	interior	Ø1.9164±0.0449	0.0853	0.0300	0.0310	0.0300	1451	0.0020	1.5569	0.9582
c08	interior	Ø1.6672±0.0588	0.1156	0.0400	0.0390	0.0400	1132	0.0020	1.0583	0.8336
c09	interior	Ø1.1392±0.0640	0.1094	0.0393	0.0365	0.0389	698	0.0020	0.5598	0.5696

Table 1: Detailed circularity measurements at selected samples of MV006.

Figure 5 to Figure 13 shows a detailed plots of each circularity measurement.

<sup>8</sup>Sample diameter Ø± maximum measured deviation from measured radius

<sup>9</sup>Root mean square deviation (RMSD) also called Root mean square error (RMSE)

<sup>10</sup>Median absolute deviation

<sup>11</sup>Median sample radius from z-axis

Graphical overview of circularity measurement c01

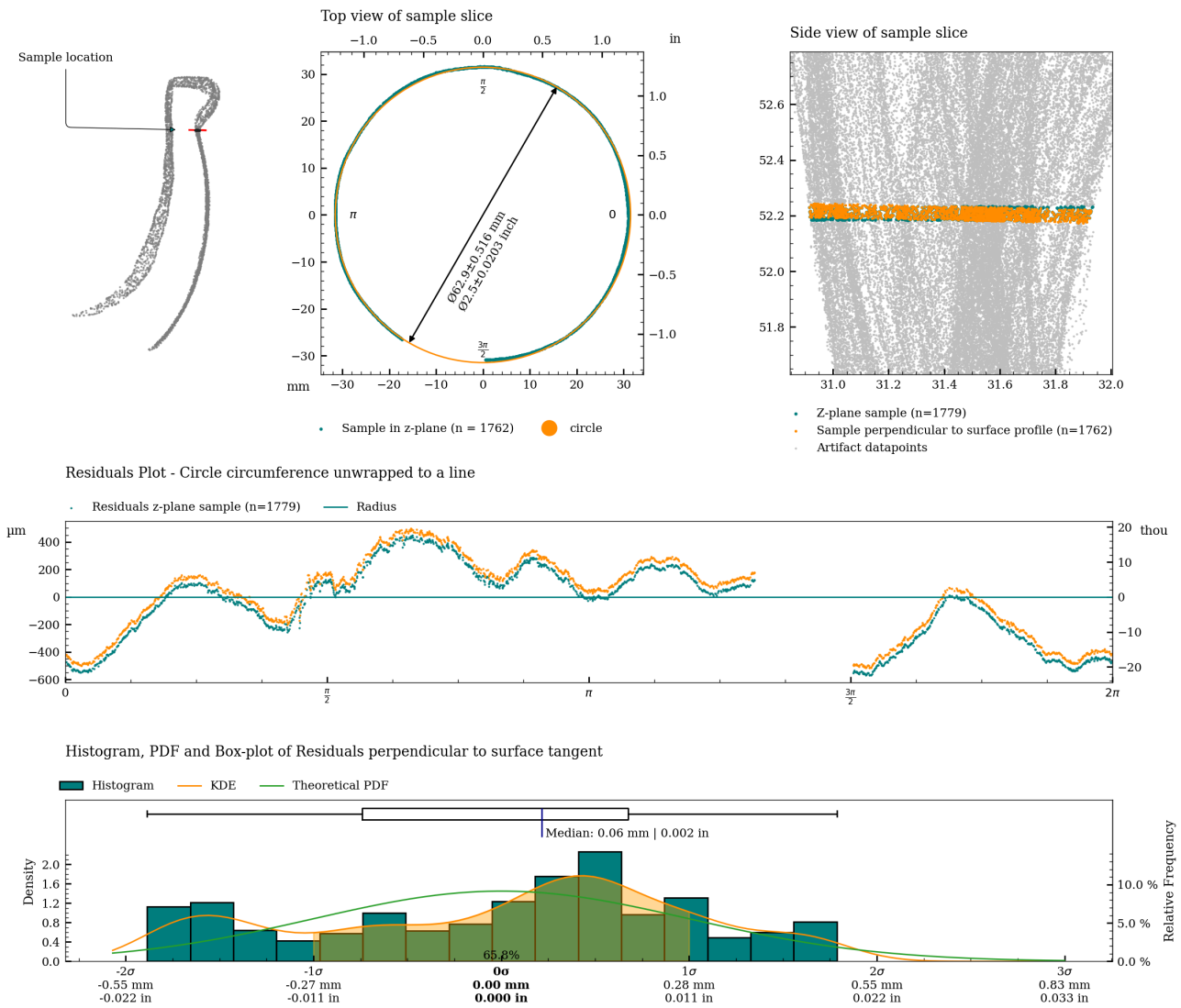


Figure 5: Charts with statistics for the measurement of c01.

Graphical overview of circularity measurement c02

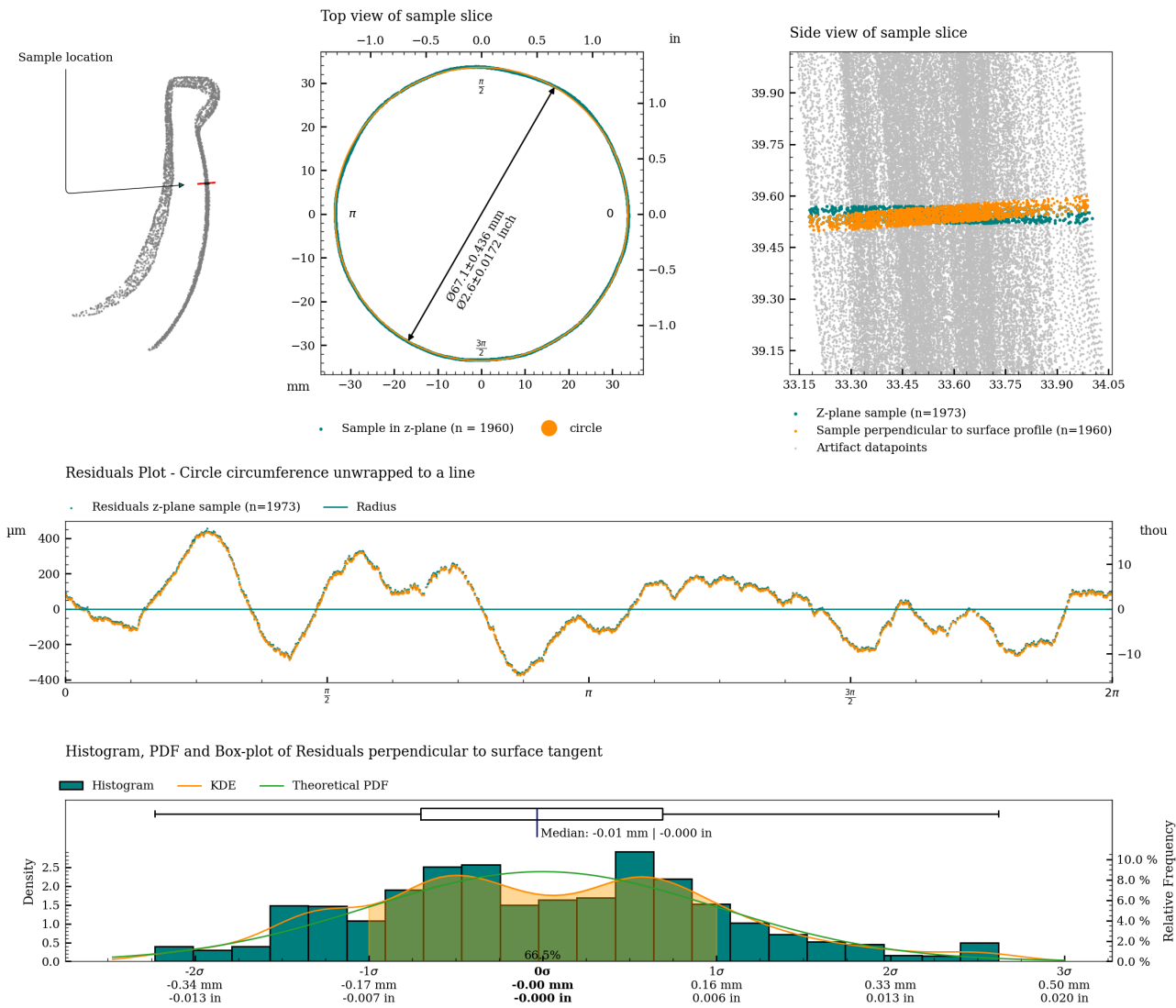


Figure 6: Charts with statistics for the measurement of c02.

Graphical overview of circularity measurement c03

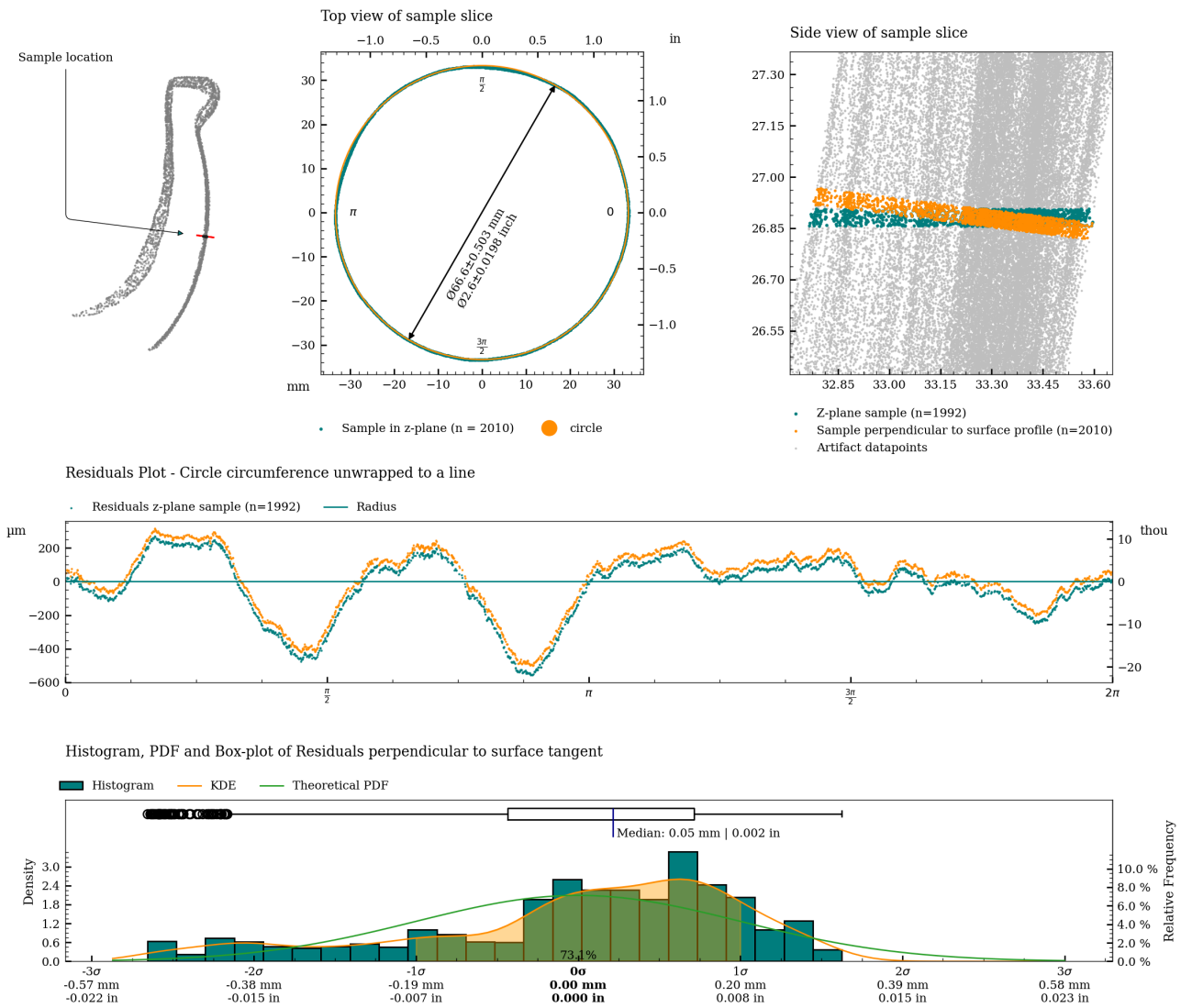


Figure 7: Charts with statistics for the measurement of c03.

Graphical overview of circularity measurement c04

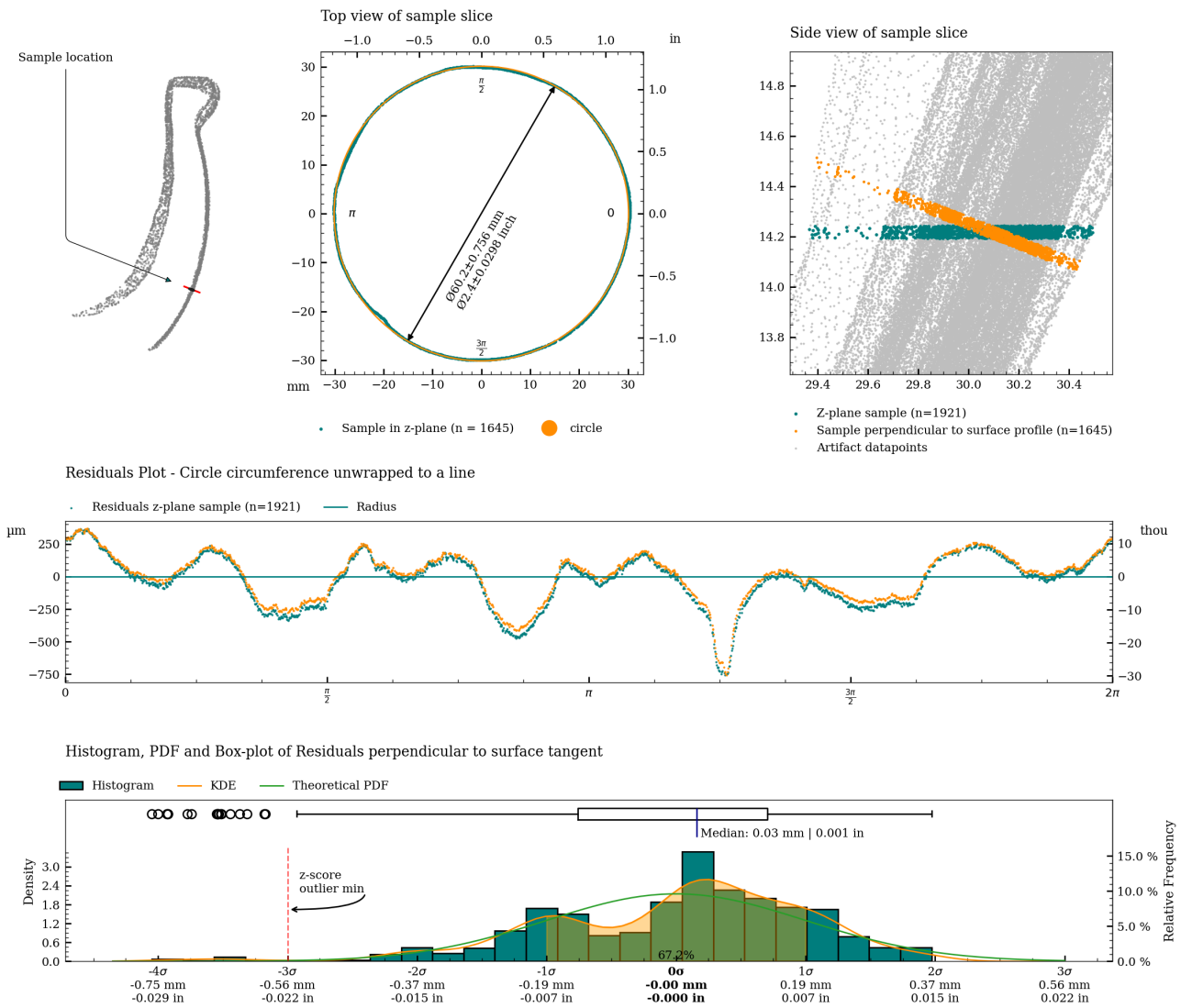


Figure 8: Charts with statistics for the measurement of c04.

Graphical overview of circularity measurement c05

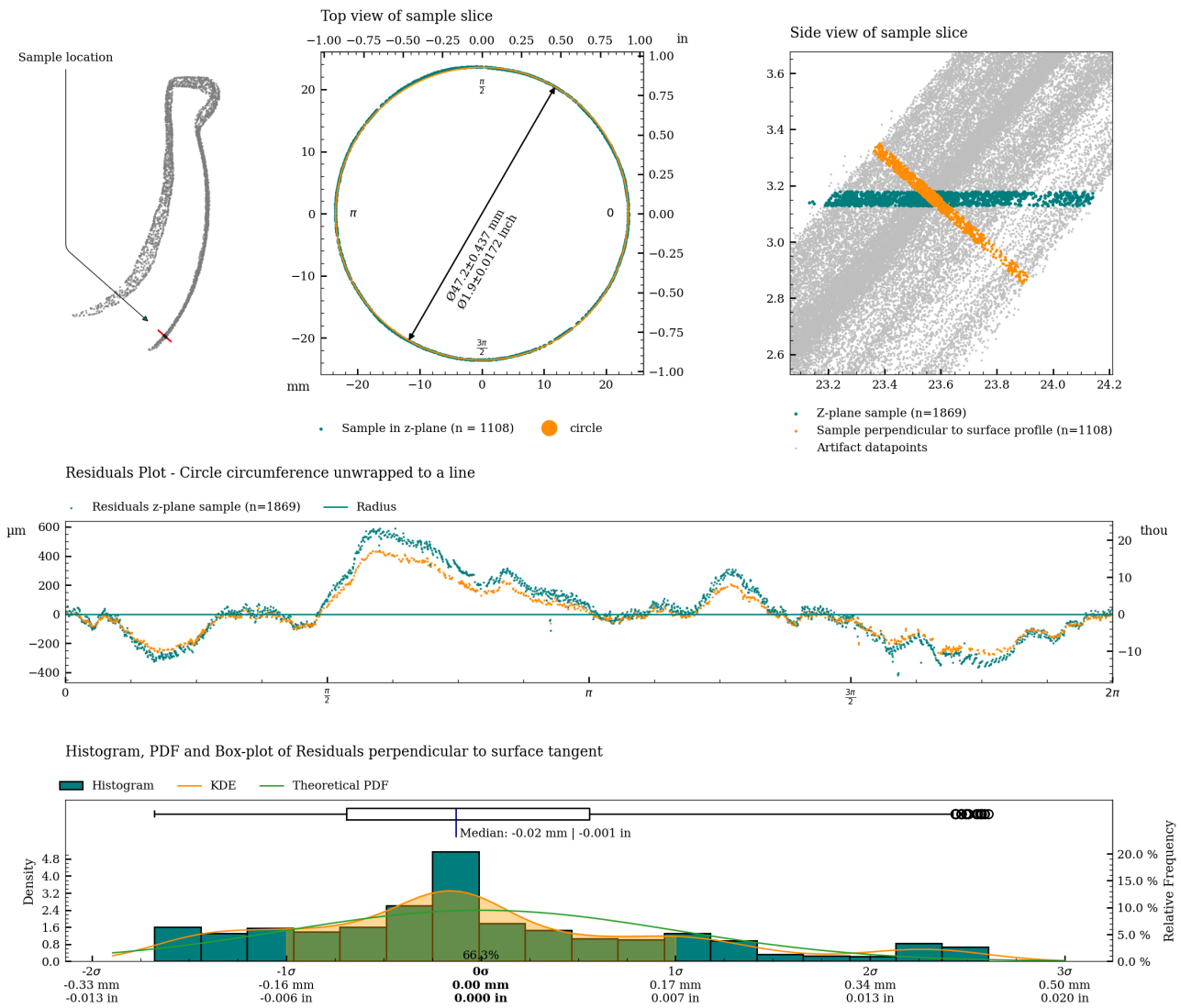


Figure 9: Charts with statistics for the measurement of c05.

Graphical overview of circularity measurement c06

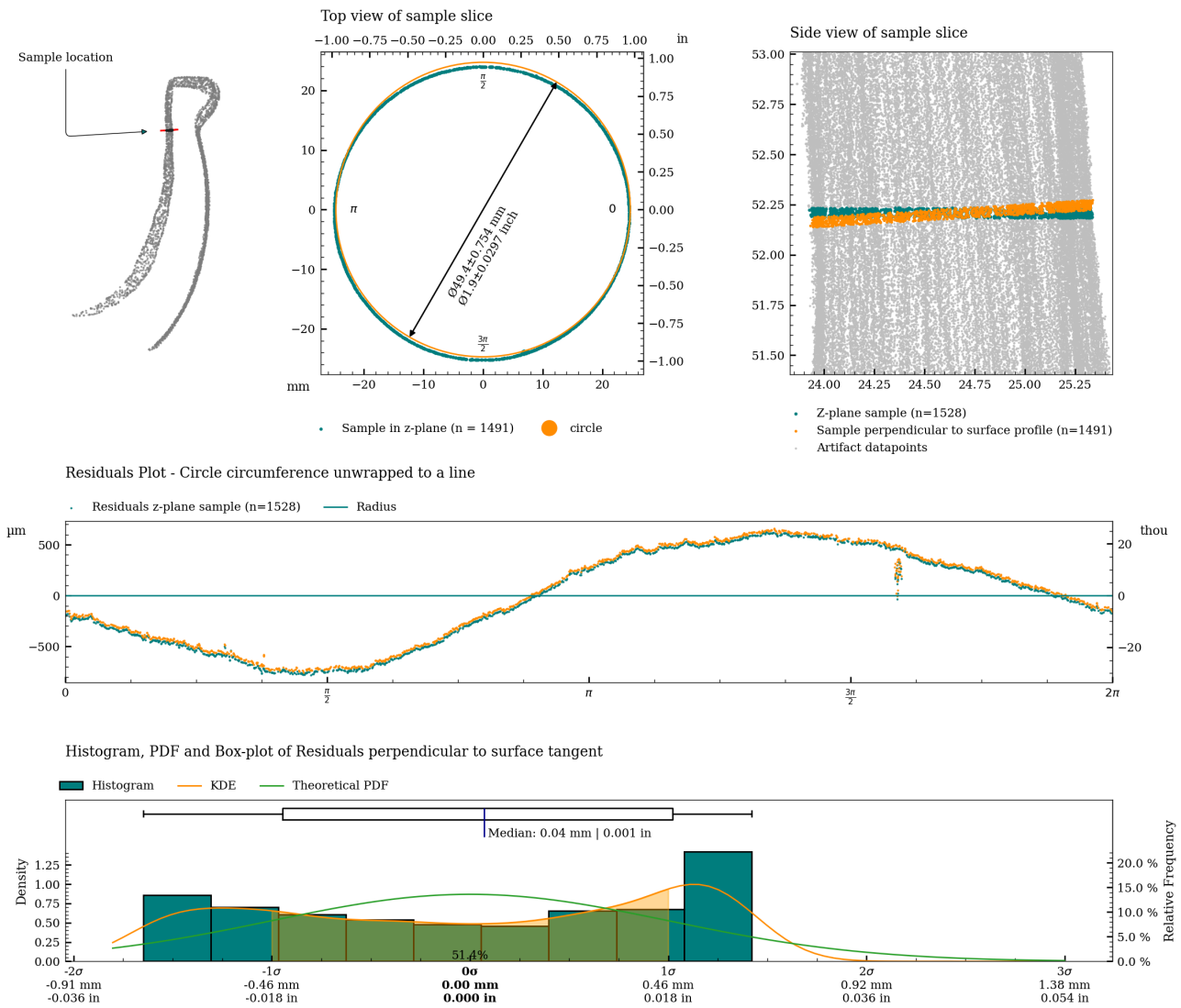
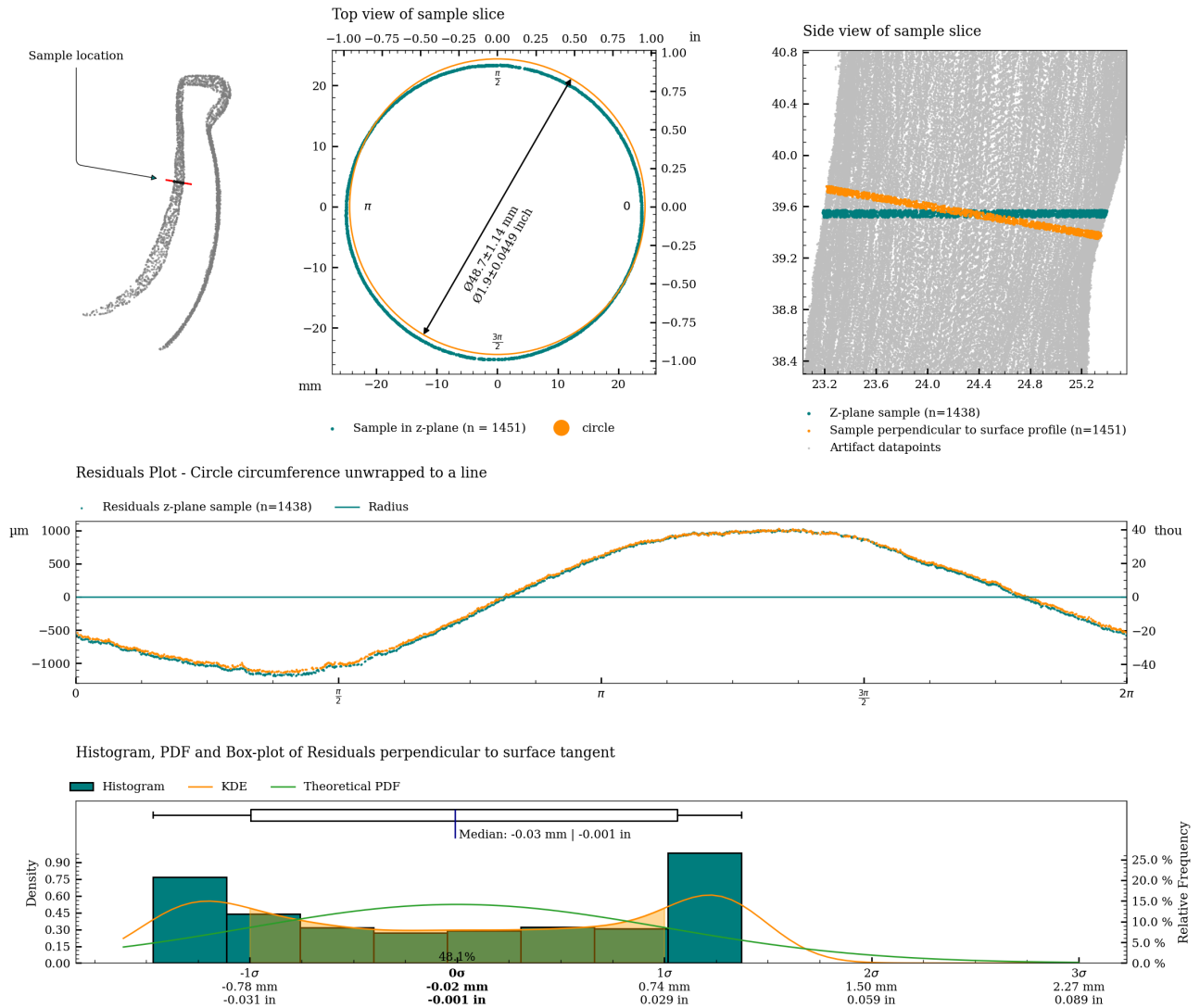


Figure 10: Charts with statistics for the measurement of c06.

## Graphical overview of circularity measurement c07



Graphical overview of circularity measurement c08

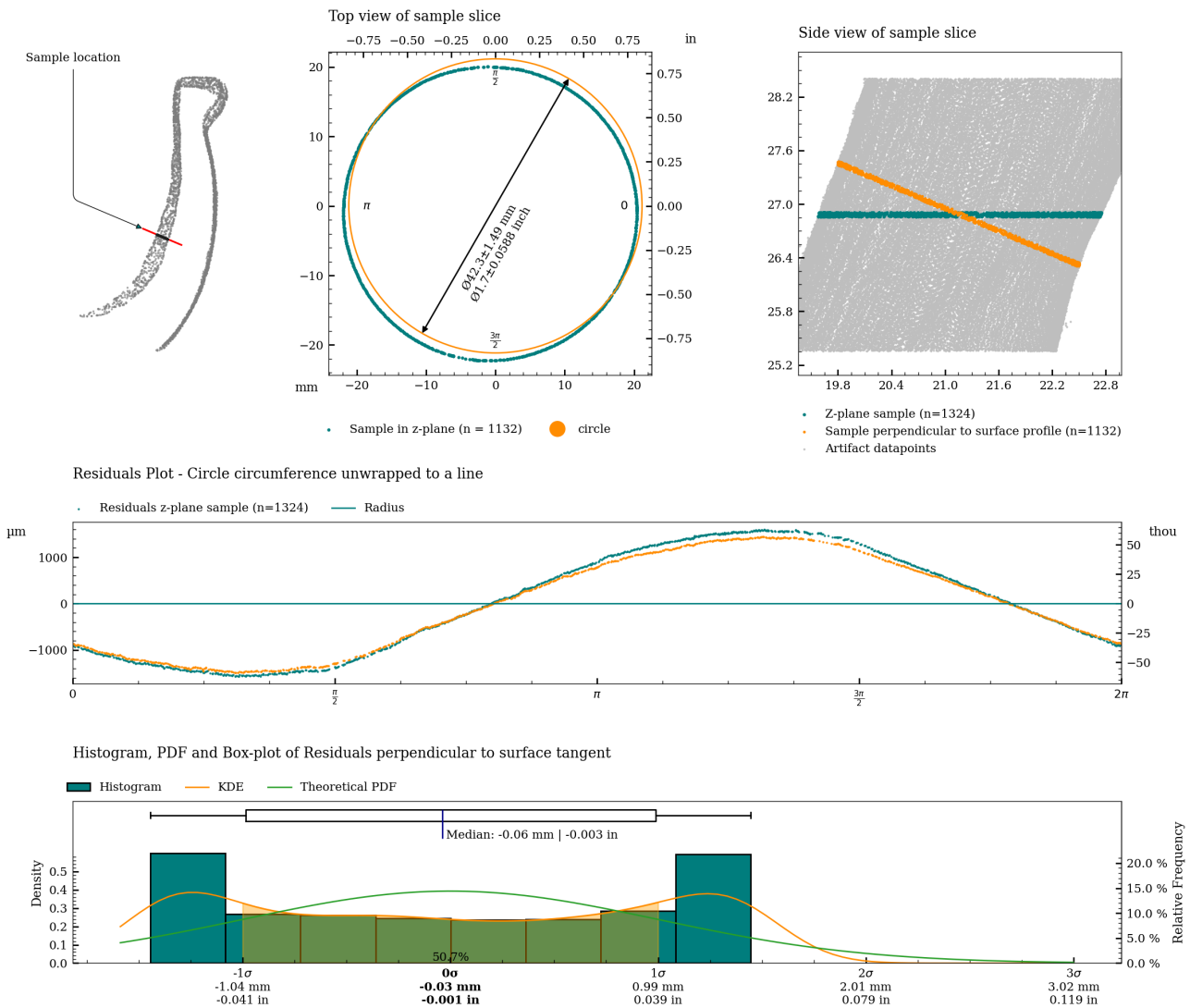


Figure 12: Charts with statistics for the measurement of c08.

## Graphical overview of circularity measurement c09

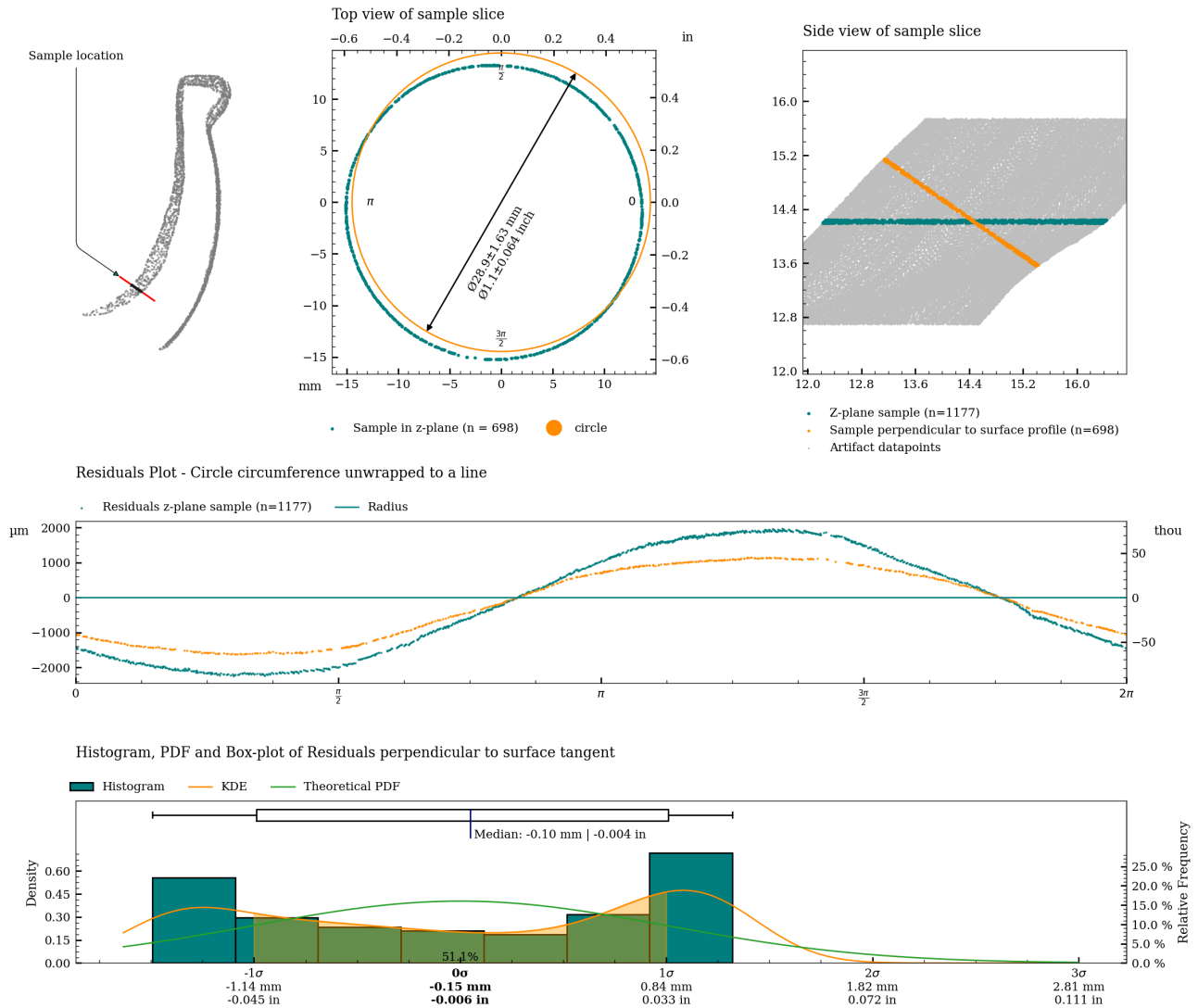


Figure 13: Charts with statistics for the measurement of c09.

Table 2 shows statistical measures of the circularity of the vessel, measured along the full height (damaged parts may reduce the measurement area).

Metric											
Area	Range			Standard Deviation			Median Absolute Deviation			Slices	Slice height
	Median	Min.	Max.	Median	Min.	Max.	Median	Min.	Max.		
	mm	mm	mm	mm	mm	mm	mm	mm	mm		
Exterior	0.860	0.567	3.058	0.195	0.143	0.807	0.012	0.070	0.830	1207	0.050
Interior	2.016	0.559	3.597	0.640	0.148	1.101	0.179	0.085	1.104	1057	0.050

Imperial											
Area	Range			Standard Deviation			Median Absolute Deviation			Slices	Slice height
	Median	Min.	Max.	Median	Min.	Max.	Median	Min.	Max.		
	in	in	in	in	in	in	in	in	in		
Exterior	0.860	0.567	3.058	0.195	0.143	0.807	0.012	0.070	0.830	1207	0.050
Interior	2.016	0.559	3.597	0.640	0.148	1.101	0.179	0.085	1.104	1057	0.050

Table 2: Perpendicular Circularity analysis of MV006.

Circularity analysis of exterior surface

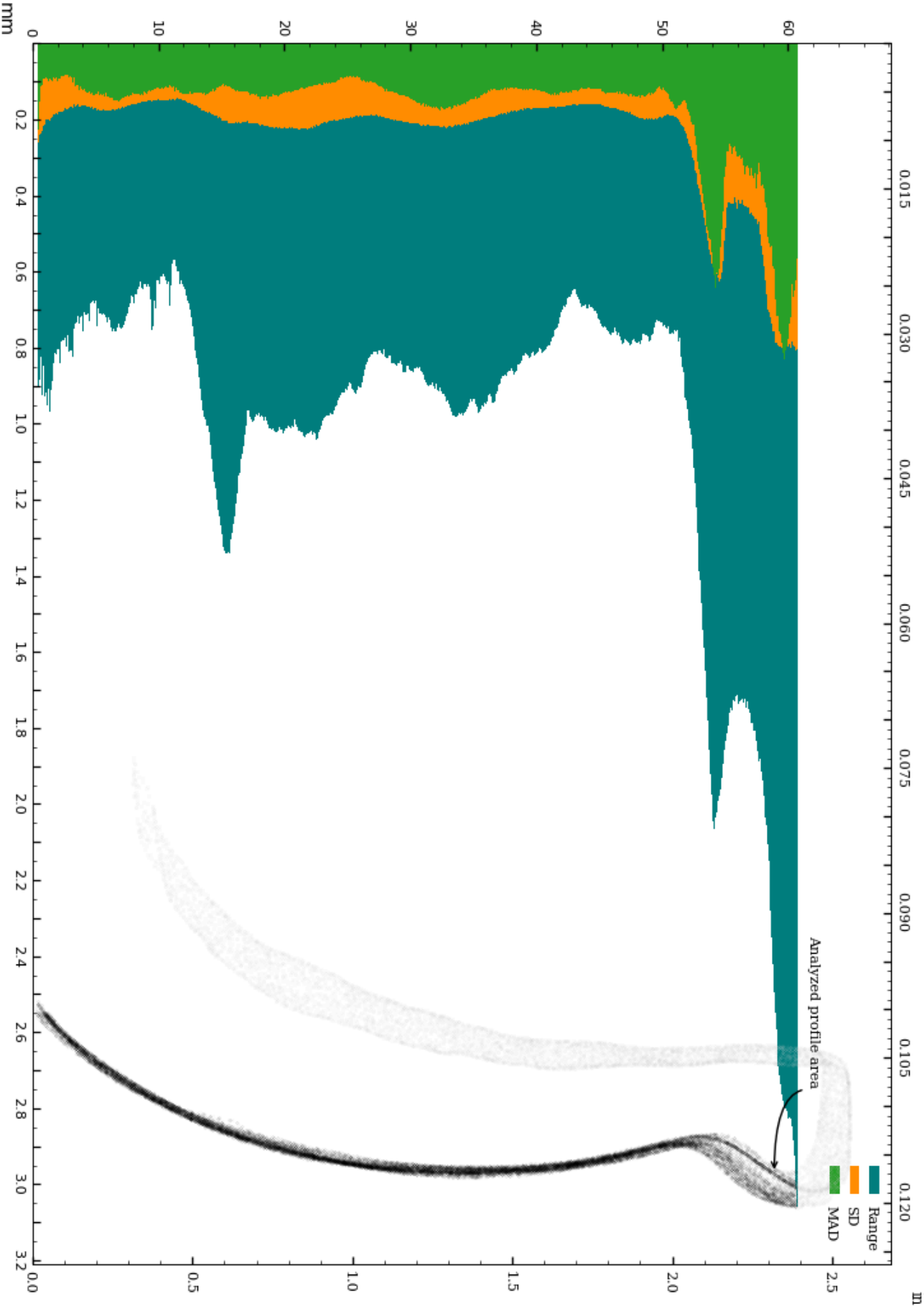


Figure 14: Circularity of exterior surface.

Circularity analysis of exterior surface, Standard Deviation and Median Absolute Deviation

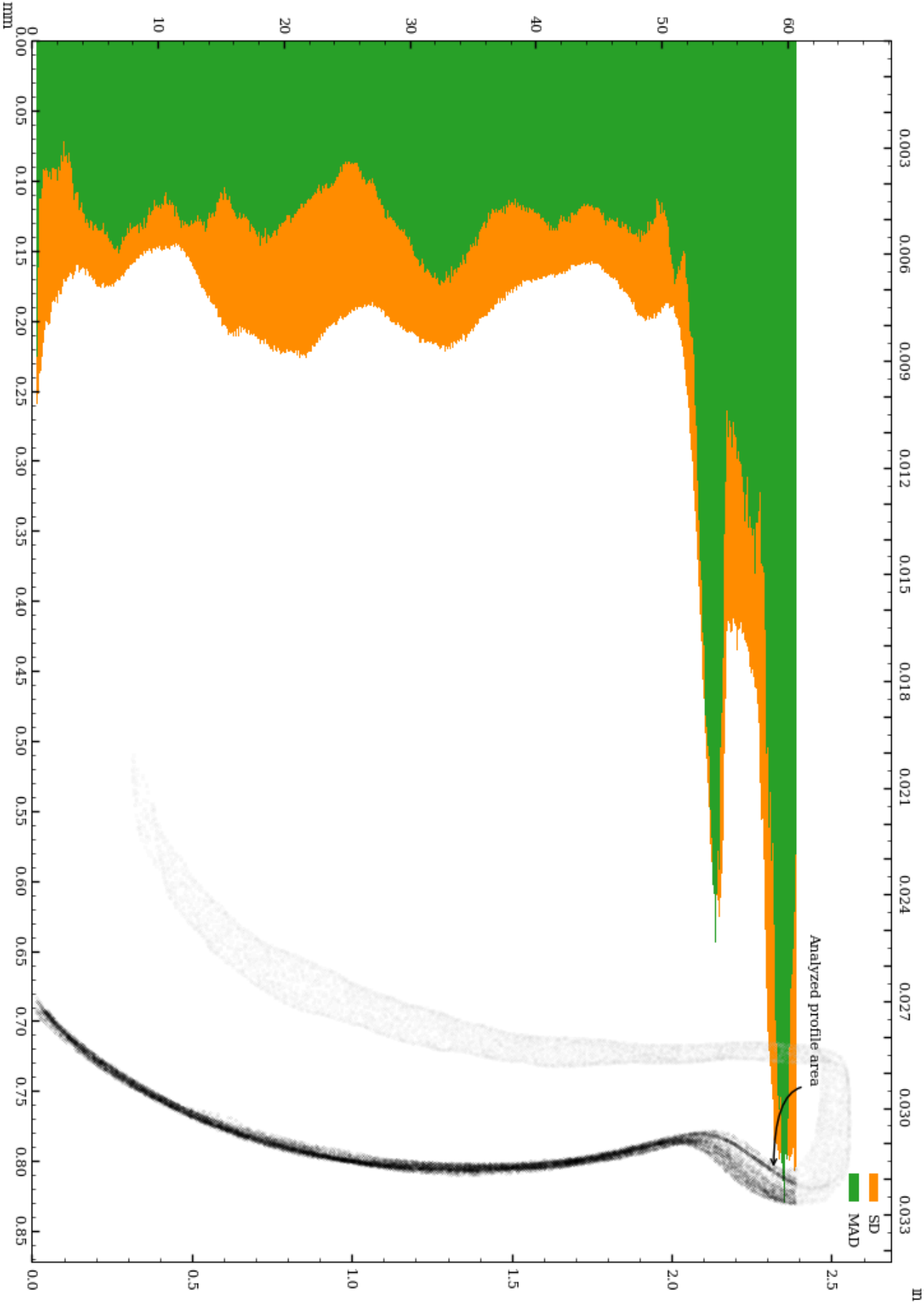


Figure 15: Vessel circularity of exterior surface, standard deviation and median absolute deviation.

The distributions of the circularity measurements across 1207 slices of the exterior surface are shown below.

### Range measurement distribution across 1207 slices of exterior surface

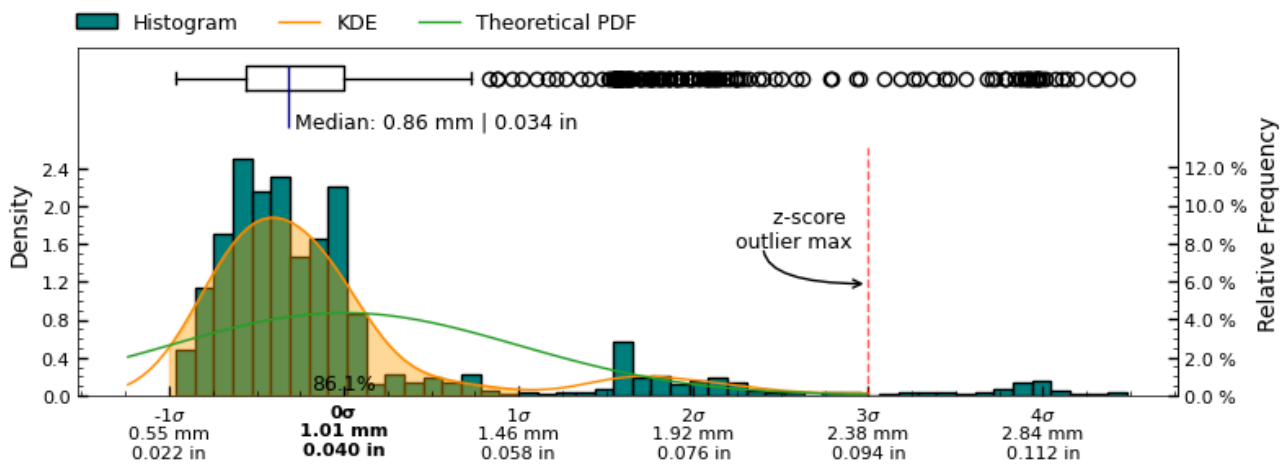


Figure 16: Range measurement distribution across measured slices of exterior surface

### Standard deviation measurement distribution across 1207 slices of exterior surface

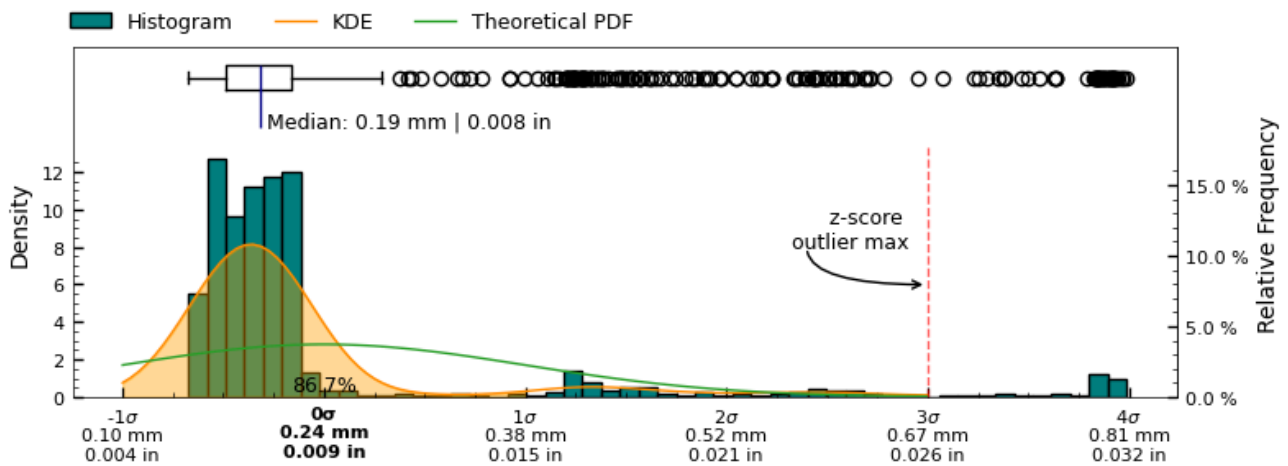


Figure 17: Standard deviation measurement distribution across measured slices of " + exterior + " surface

### Median absolute deviation measurement distribution across 1207 slices of exterior surface

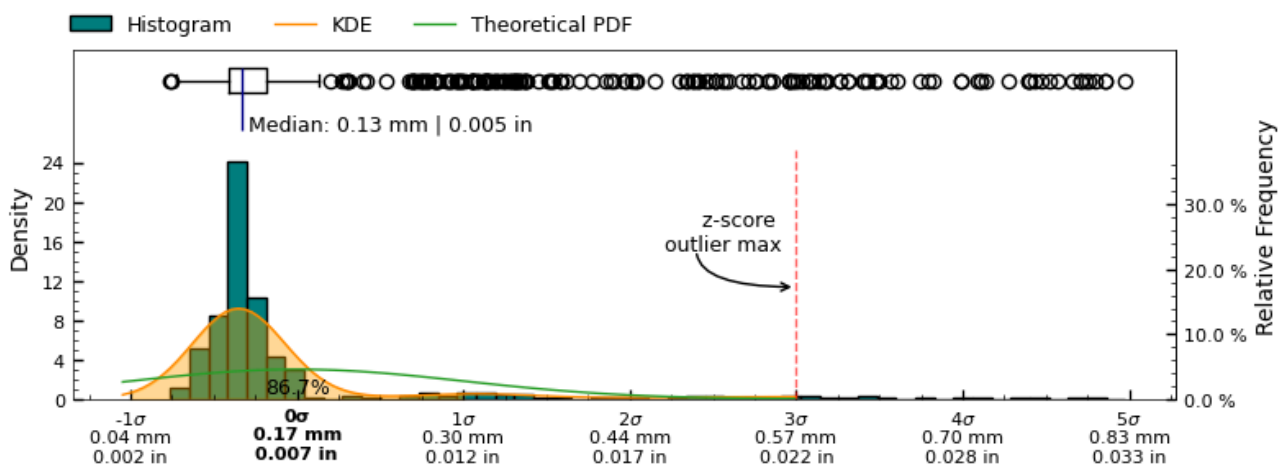


Figure 18: Median absolute deviation measurement distribution across measured slices of exterior surface

Circularity analysis of interior surface

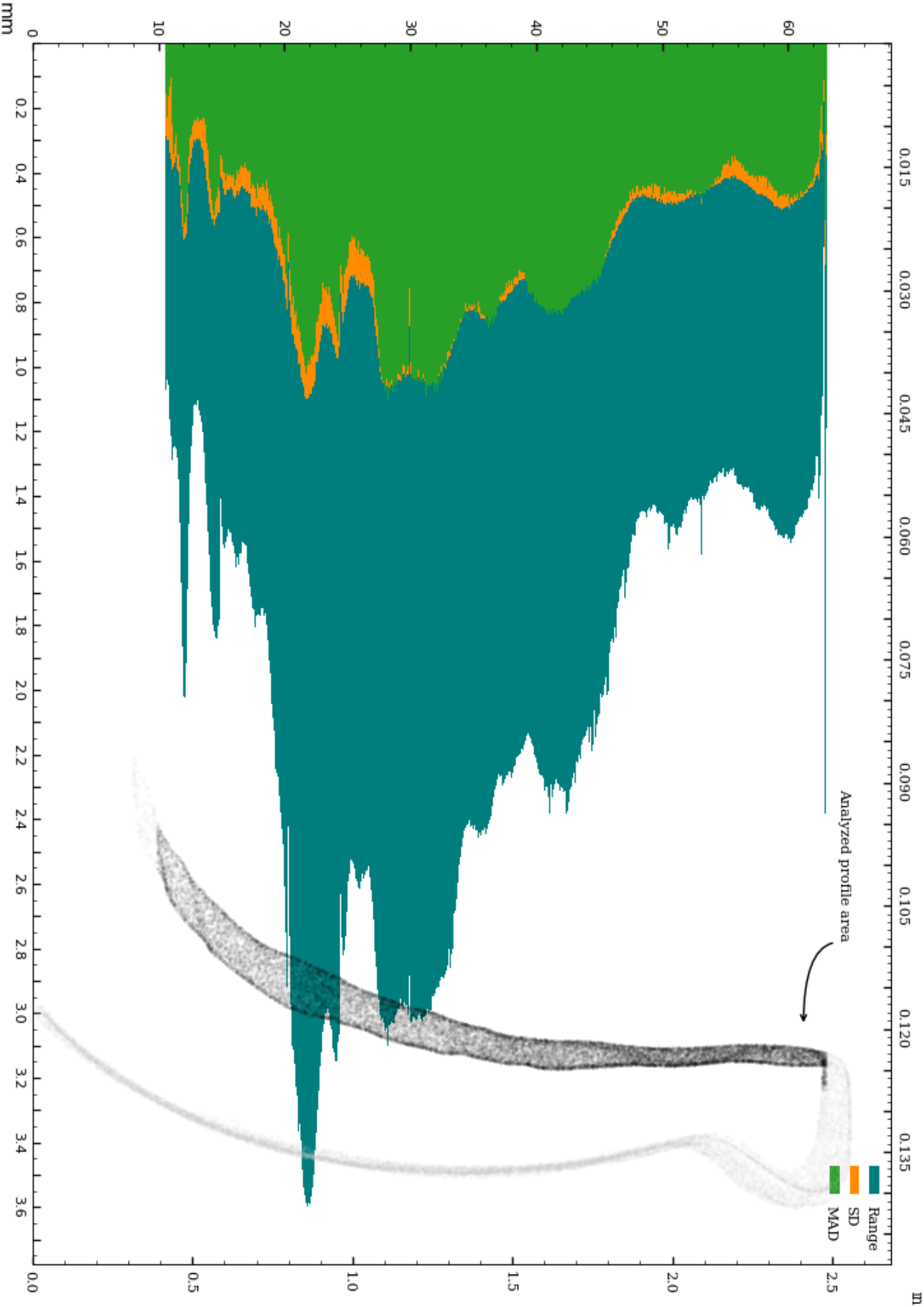


Figure 19: Circularity of interior surface.

Circularity analysis of interior surface, Standard Deviation and Median Absolute Deviation

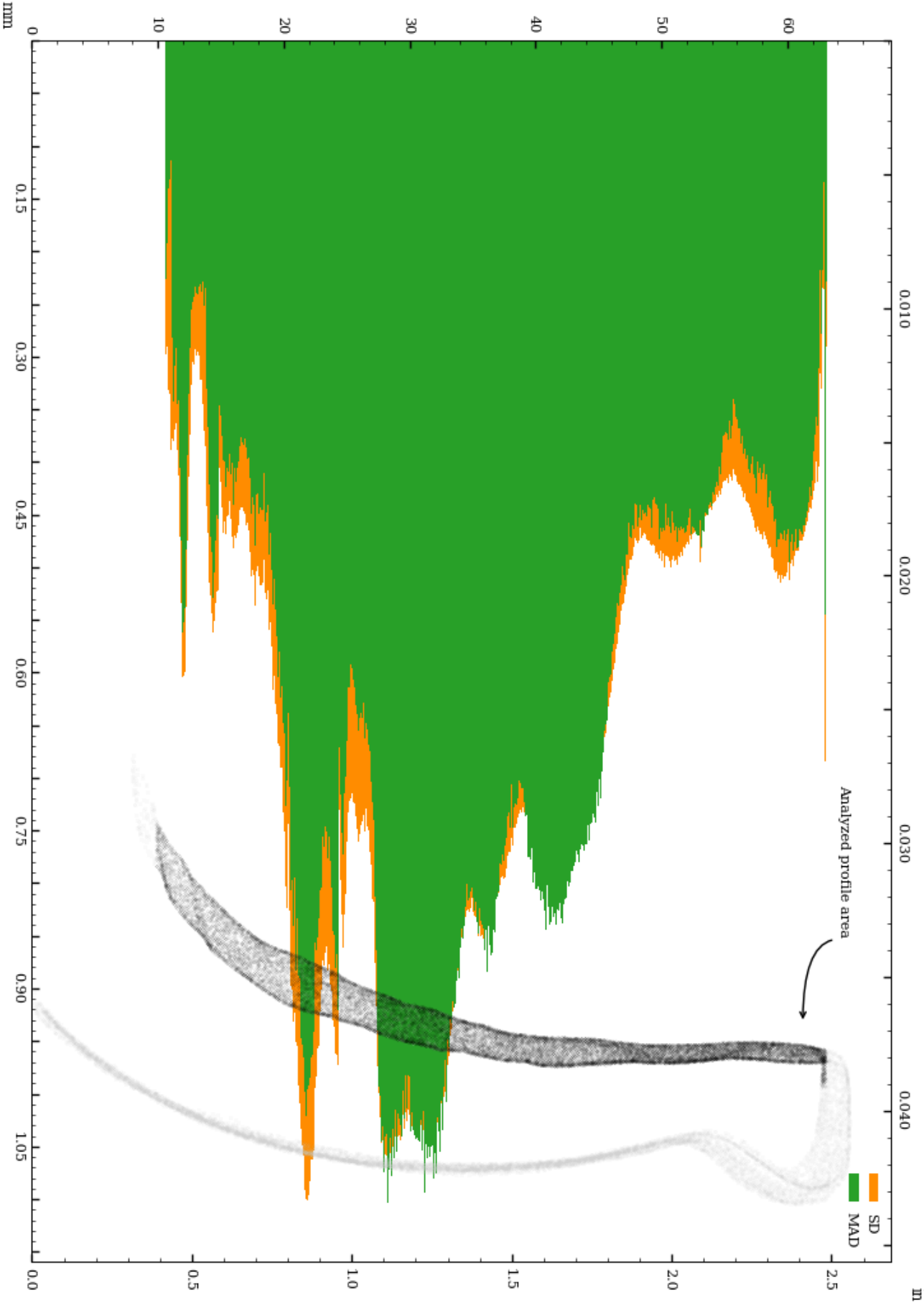


Figure 20: Vessel circularity of interior surface, standard deviation and median absolute deviation.

The distributions of the circularity measurements across 1057 slices of the interior surface are shown below.

### Range measurement distribution across 1057 slices of interior surface

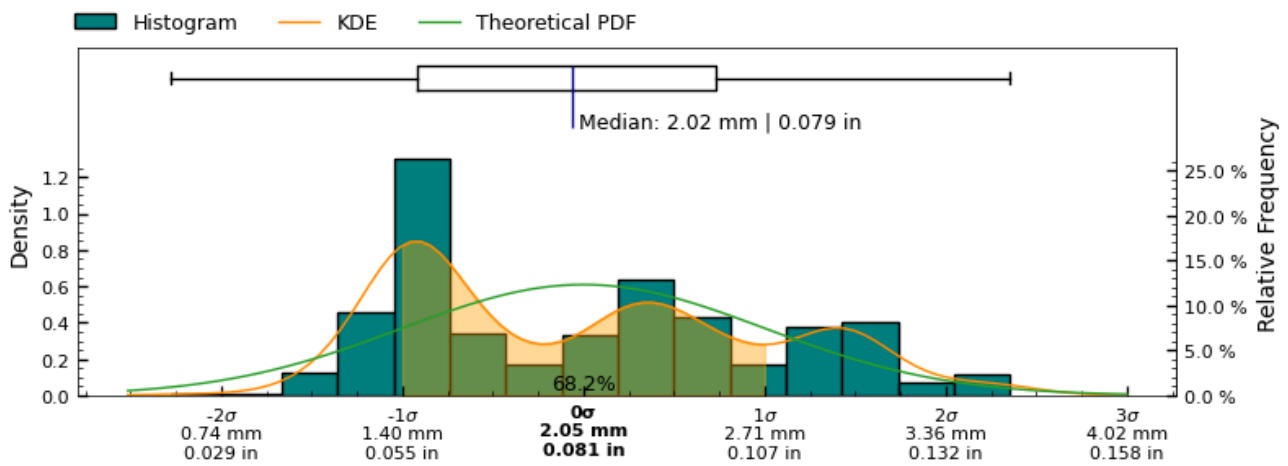


Figure 21: Range measurement distribution across measured slices of interior surface

### Standard deviation measurement distribution across 1057 slices of interior surface

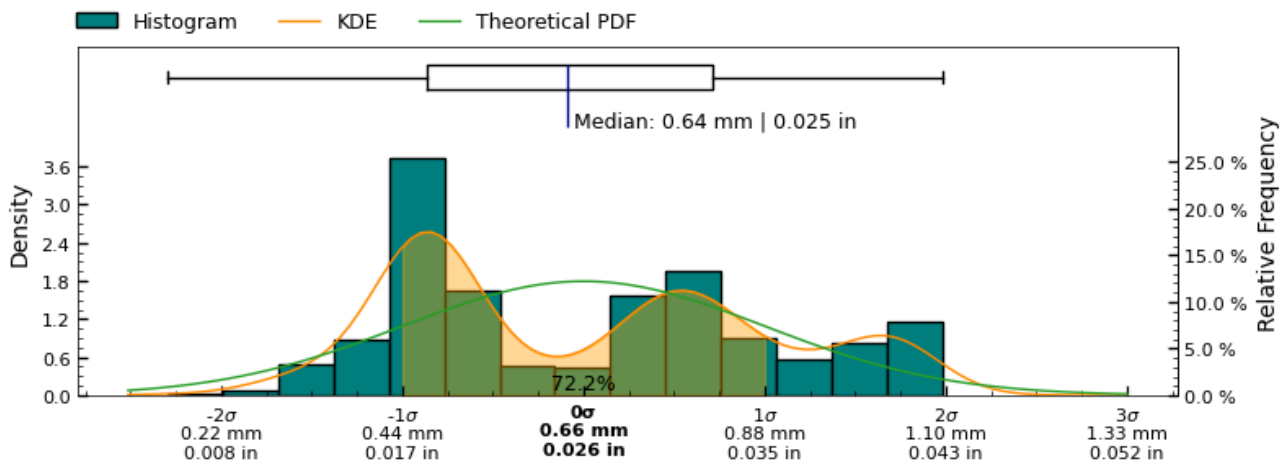


Figure 22: Standard deviation measurement distribution across measured slices of " + interior + " surface

### Median absolute deviation measurement distribution across 1057 slices of interior surface

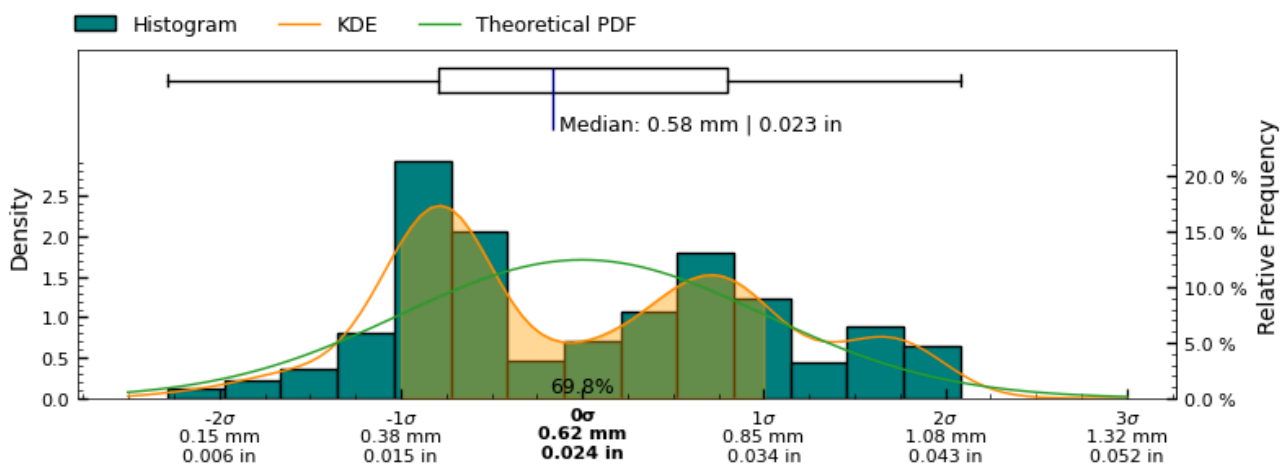


Figure 23: Median absolute deviation measurement distribution across measured slices of interior surface

## Concentricity

The concentricity metric describes the deviation in the center-point of the referenced features. As such, it is a measure to determine if several features of the object share the same center point/axis, and how closely. See Figure 24 for a visual representation of this metric.

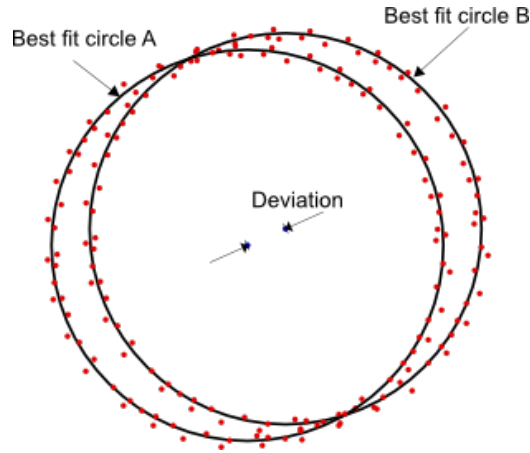


Figure 24: Concentricity measures the deviation (distance) between the center of two circles.

Determination of concentricity has been carried out by establishing the best fit circles of sample slices, using RANSAC (Random sample consensus) algorithm for outlier detection of a least squares circle regression on the scanned data-points at each cross-section, to estimate centers of each cross-section.

The concentricity between both the interior and exterior circular cross-sections is explored for cross-section measurements with the same Z-coordinates.

Additionally, the concentricity between each cross-section measurement defined in Figure 4 and the datum axis  $(x, y) = (0, 0)$  has been calculated to establish the deviation of the feature center from the datum axis.

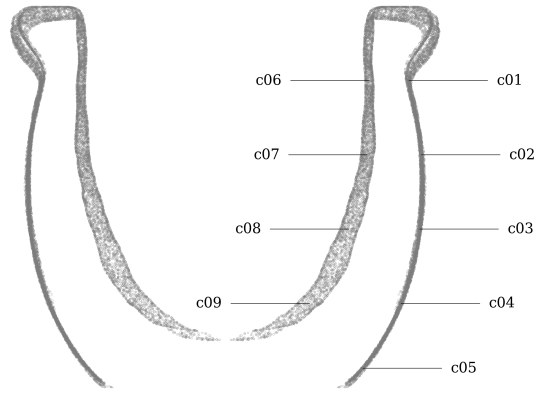


Figure 25: Concentricity measurement sample location on MV006.

### Metric

Tag	Reference	Deviation	Sample size	Circle fit residuals analysis for sample listed in Tag column						
				Range full	Range inliers	SD full	SD inliers	MAD full	MAD inliers	Center (x,y)
		mm		mm	mm	mm	mm	mm	mm	μm
c01	z-axis	0.304	1762	1.012	1.012	0.276	0.276	0.199	0.199	−259, 160
c02	z-axis	0.066	1960	0.812	0.812	0.167	0.167	0.114	0.114	−3, 66
c03	z-axis	0.061	2010	0.818	0.776	0.191	0.175	0.103	0.098	−10, −60
c04	z-axis	0.082	1645	1.124	0.915	0.187	0.172	0.124	0.122	82, 9
c05	z-axis	0.137	1108	0.714	0.714	0.167	0.167	0.099	0.099	−114, 75
c06	z-axis	0.638	1491	1.411	1.411	0.460	0.462	0.455	0.456	−196, −607
c07	z-axis	1.041	1451	2.165	2.165	0.763	0.763	0.785	0.785	−556, −880
c08	z-axis	1.315	1132	2.937	2.937	1.017	1.011	0.992	0.977	−778, −1060
c09	z-axis	1.157	698	2.778	2.778	0.988	0.988	0.970	0.970	−683, −933
c01	c06	0.770	1762	1.012	1.012	0.276	0.276	0.199	0.199	−63, 767
c02	c07	1.095	1960	0.812	0.812	0.167	0.167	0.114	0.114	553, 946
c03	c08	1.261	2010	0.818	0.776	0.191	0.175	0.103	0.098	768, 1000
c04	c09	1.214	1645	1.124	0.915	0.187	0.172	0.124	0.122	765, 942

### Imperial

Tag	Reference	Deviation	Sample size	Circle fit residuals analysis for sample listed in Tag column						
				Range full	Range inliers	SD full	SD inliers	MAD full	MAD inliers	Center (x,y)
		in		in	in	in	in	in	in	thou
c01	z-axis	0.0120	1762	0.0398	0.0398	0.0108	0.0108	0.0078	0.0078	−10.2, 6.3
c02	z-axis	0.0026	1960	0.0320	0.0320	0.0066	0.0066	0.0045	0.0045	−0.1, 2.6
c03	z-axis	0.0024	2010	0.0322	0.0305	0.0075	0.0069	0.0040	0.0039	−0.4, −2.4
c04	z-axis	0.0032	1645	0.0442	0.0360	0.0073	0.0068	0.0049	0.0048	3.2, 0.4
c05	z-axis	0.0054	1108	0.0281	0.0281	0.0066	0.0066	0.0039	0.0039	−4.5, 2.9
c06	z-axis	0.0251	1491	0.0555	0.0555	0.0181	0.0182	0.0179	0.0180	−7.7, −23.9
c07	z-axis	0.0410	1451	0.0853	0.0853	0.0300	0.0300	0.0309	0.0309	−21.9, −34.6
c08	z-axis	0.0518	1132	0.1156	0.1156	0.0400	0.0398	0.0390	0.0385	−30.6, −41.7
c09	z-axis	0.0455	698	0.1094	0.1094	0.0389	0.0389	0.0382	0.0382	−26.9, −36.7
c01	c06	0.0303	1762	0.0398	0.0398	0.0108	0.0108	0.0078	0.0078	−2.5, 30.2
c02	c07	0.0431	1960	0.0320	0.0320	0.0066	0.0066	0.0045	0.0045	21.8, 37.2
c03	c08	0.0497	2010	0.0322	0.0305	0.0075	0.0069	0.0040	0.0039	30.2, 39.4
c04	c09	0.0478	1645	0.0442	0.0360	0.0073	0.0068	0.0049	0.0048	30.1, 37.1

Table 3: Concentricity analysis of MV006.

Concentricity analysis of c01

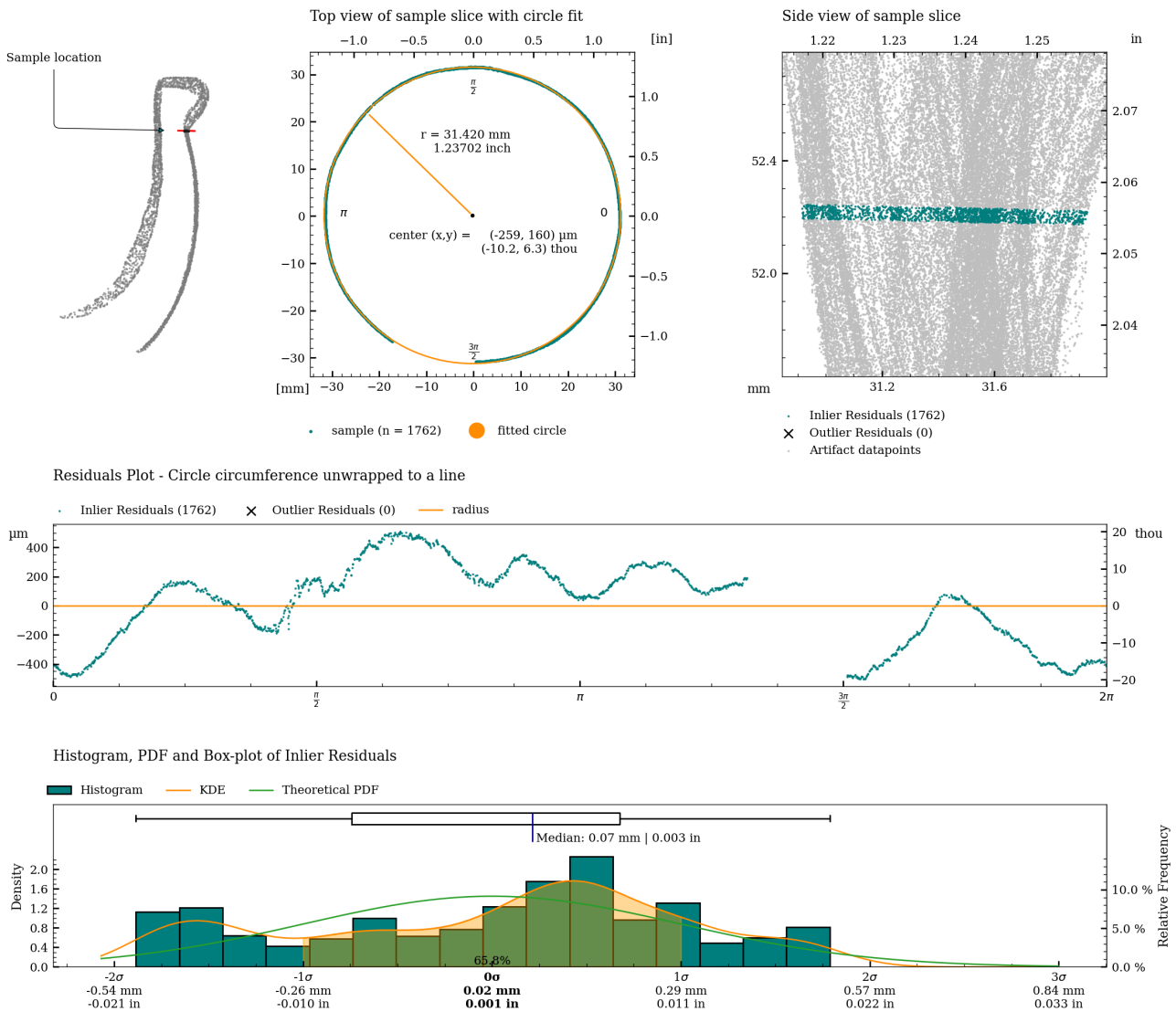


Figure 26: Detailed plot of concentricity measurement for c01.

Concentricity analysis of c02

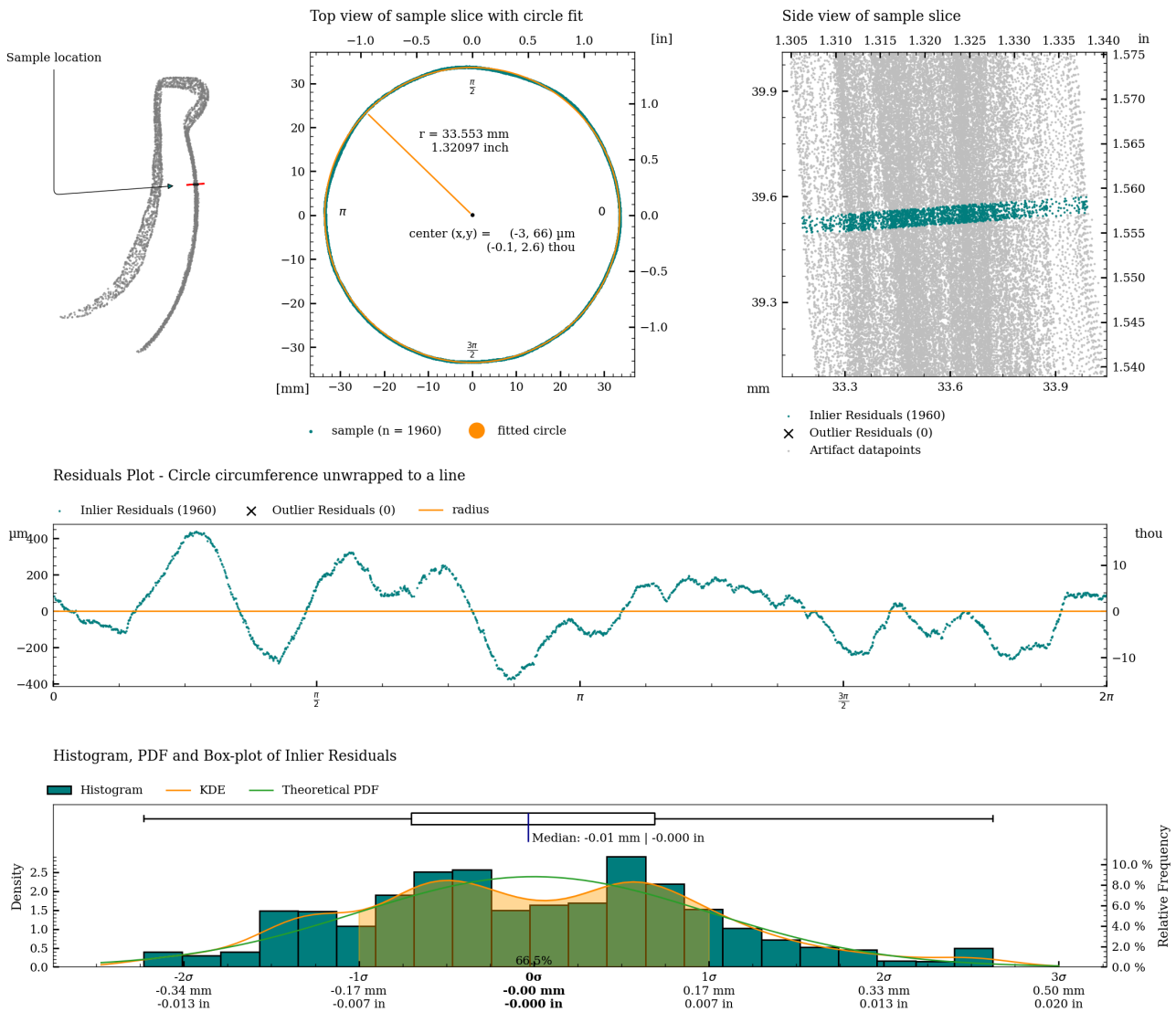


Figure 27: Detailed plot of concentricity measurement for c02.

Concentricity analysis of c03

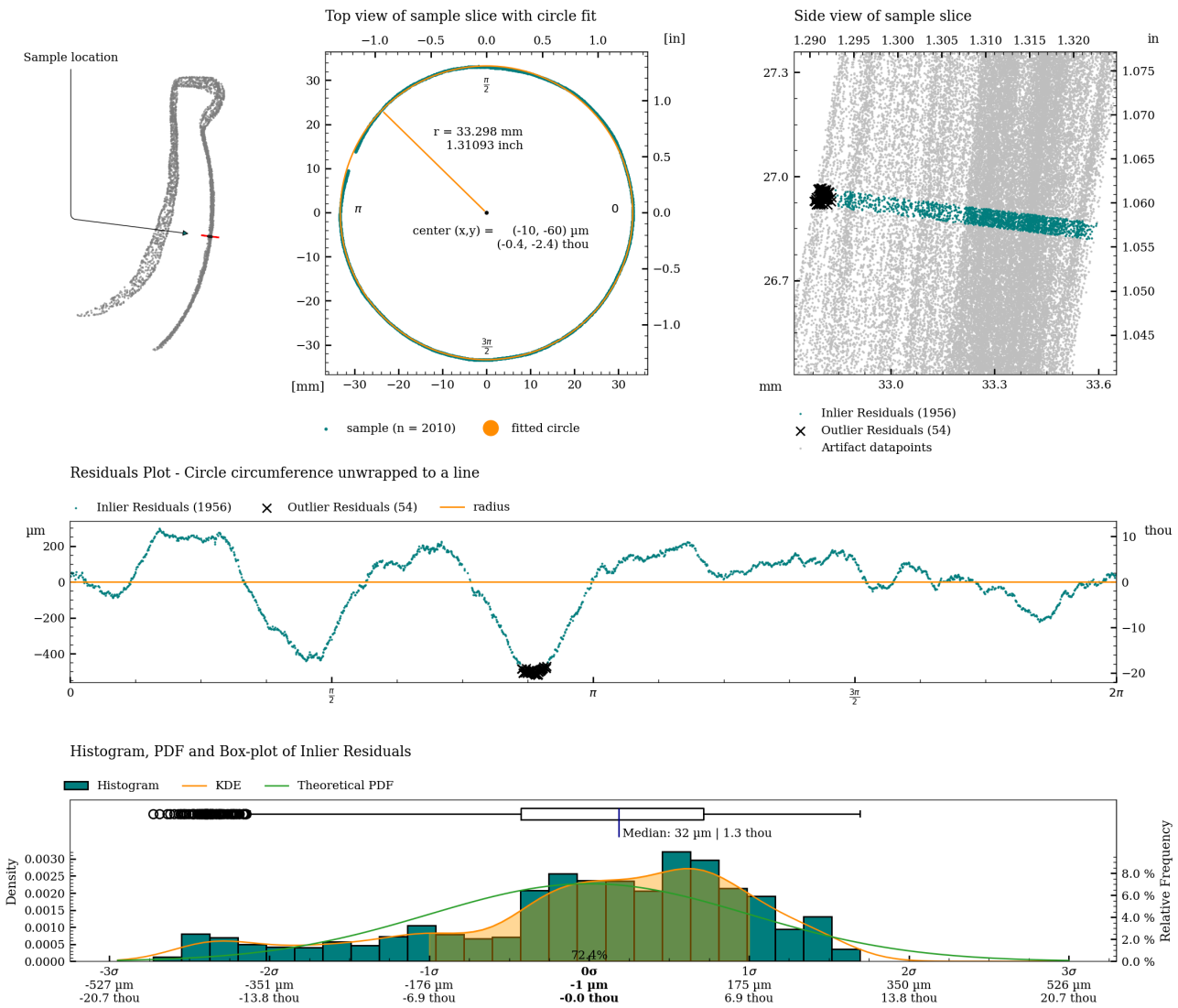
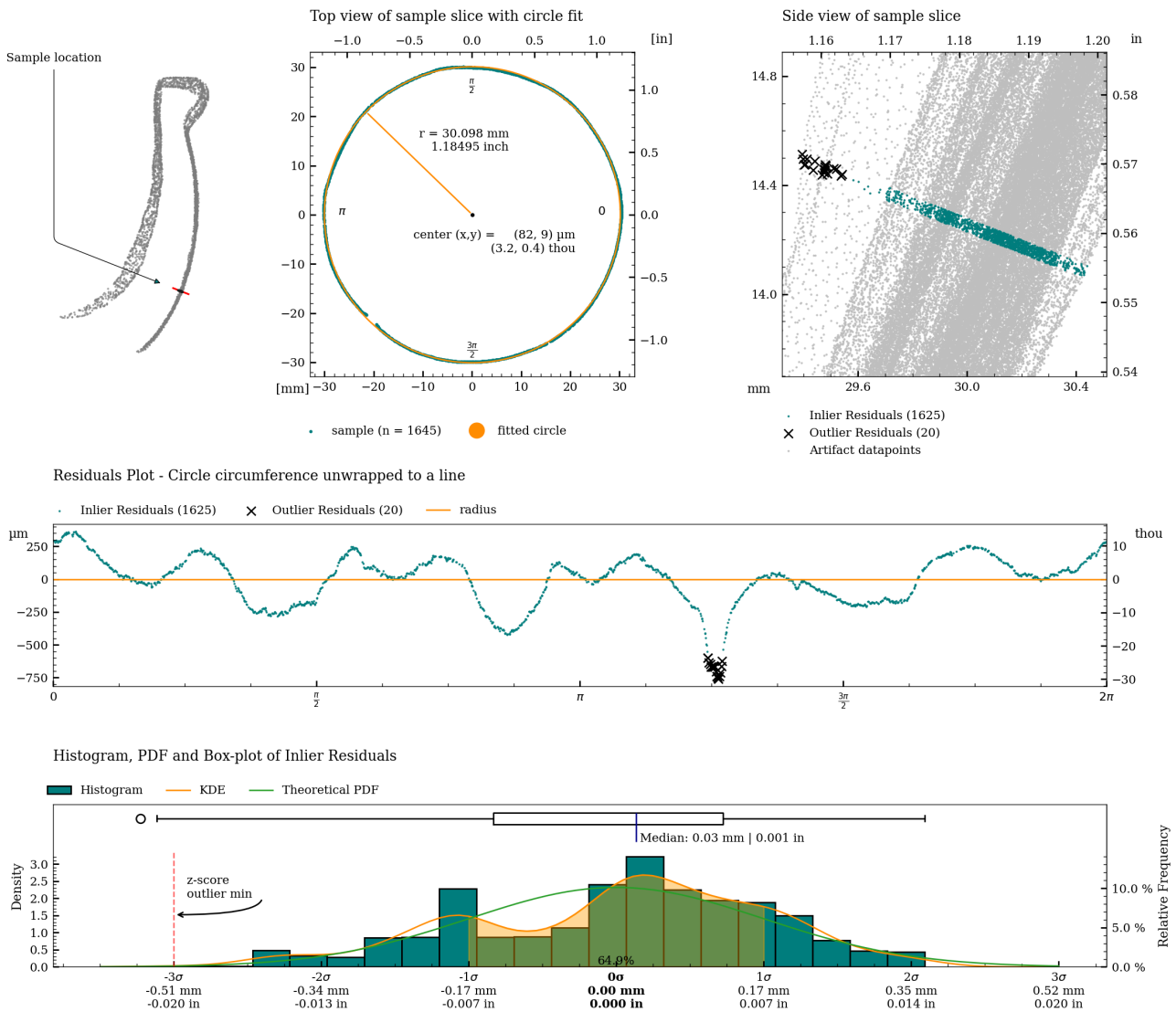


Figure 28: Detailed plot of concentricity measurement for c03.

Concentricity analysis of c04



Concentricity analysis of c05

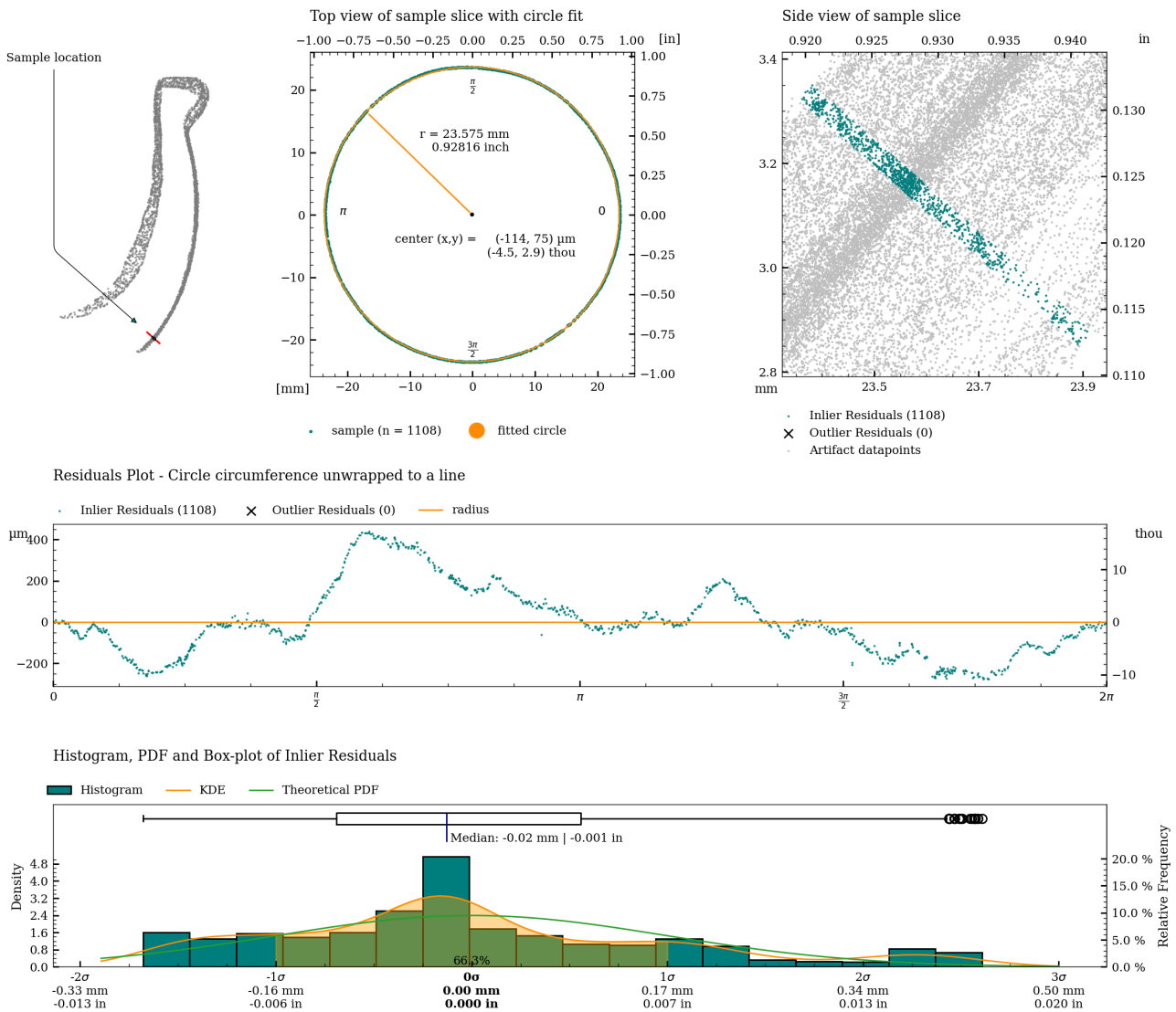


Figure 30: Detailed plot of concentricity measurement for c05.

Concentricity analysis of c06

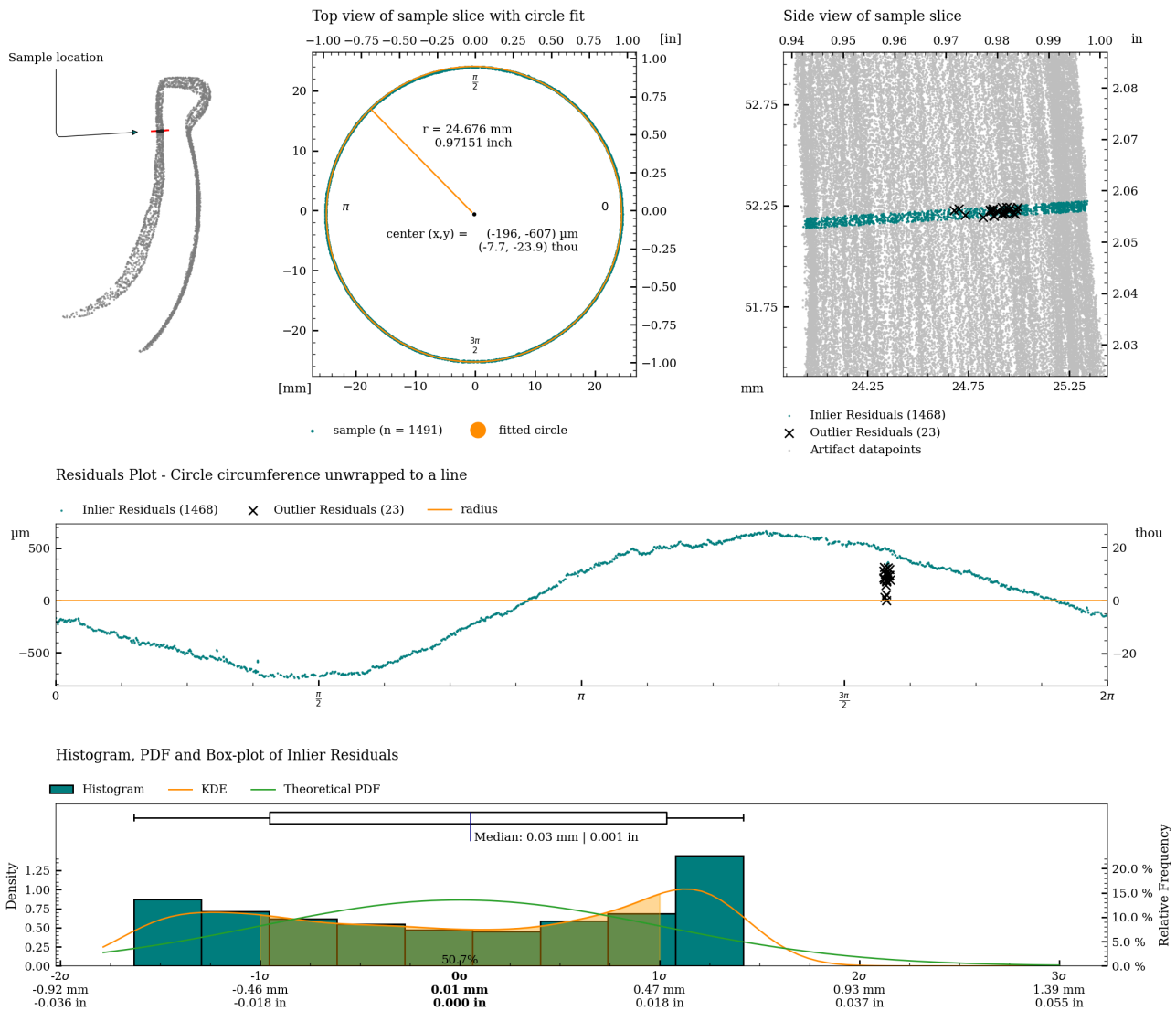


Figure 31: Detailed plot of concentricity measurement for c06.

Concentricity analysis of c07

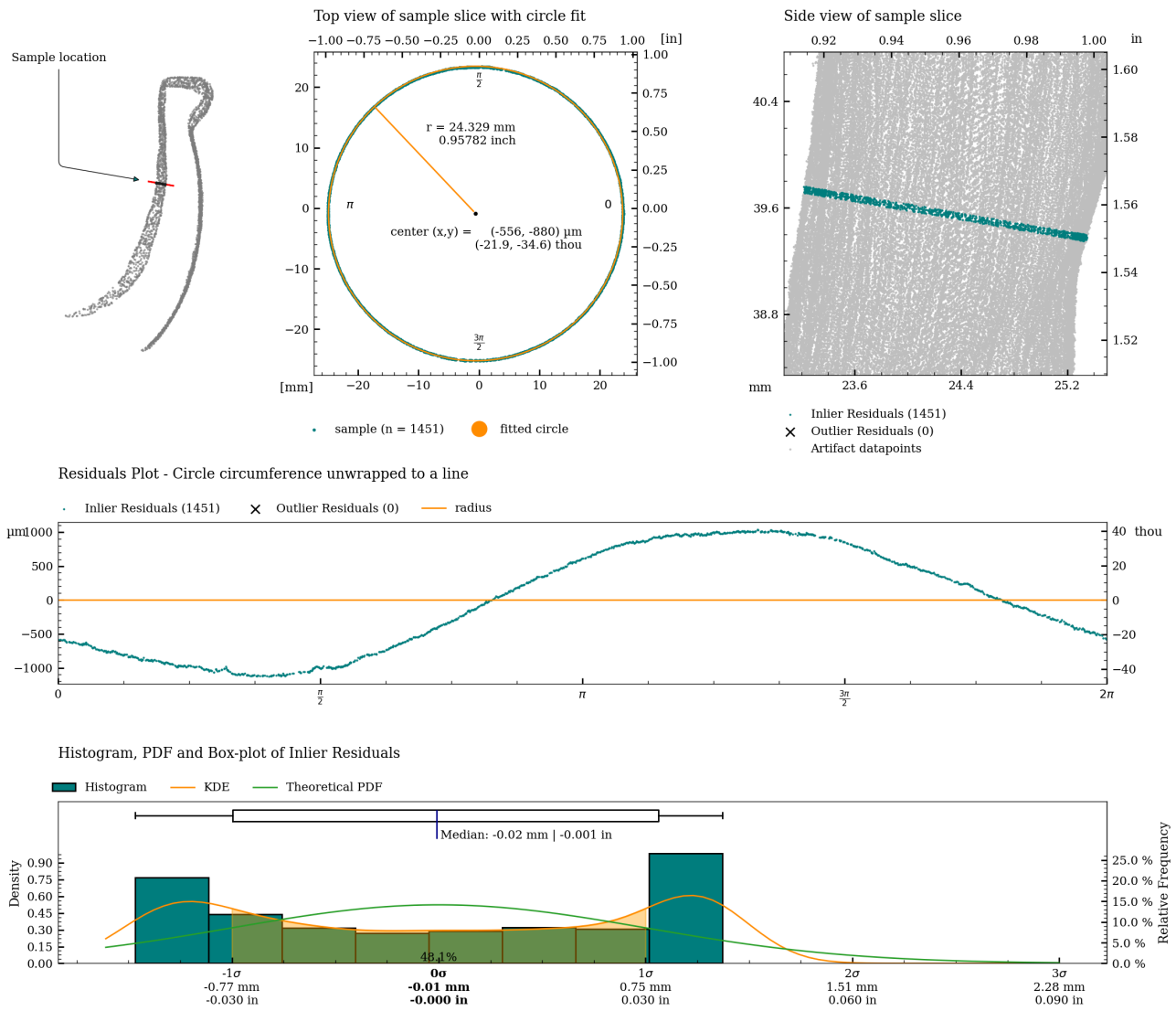


Figure 32: Detailed plot of concentricity measurement for c07.

Concentricity analysis of c08

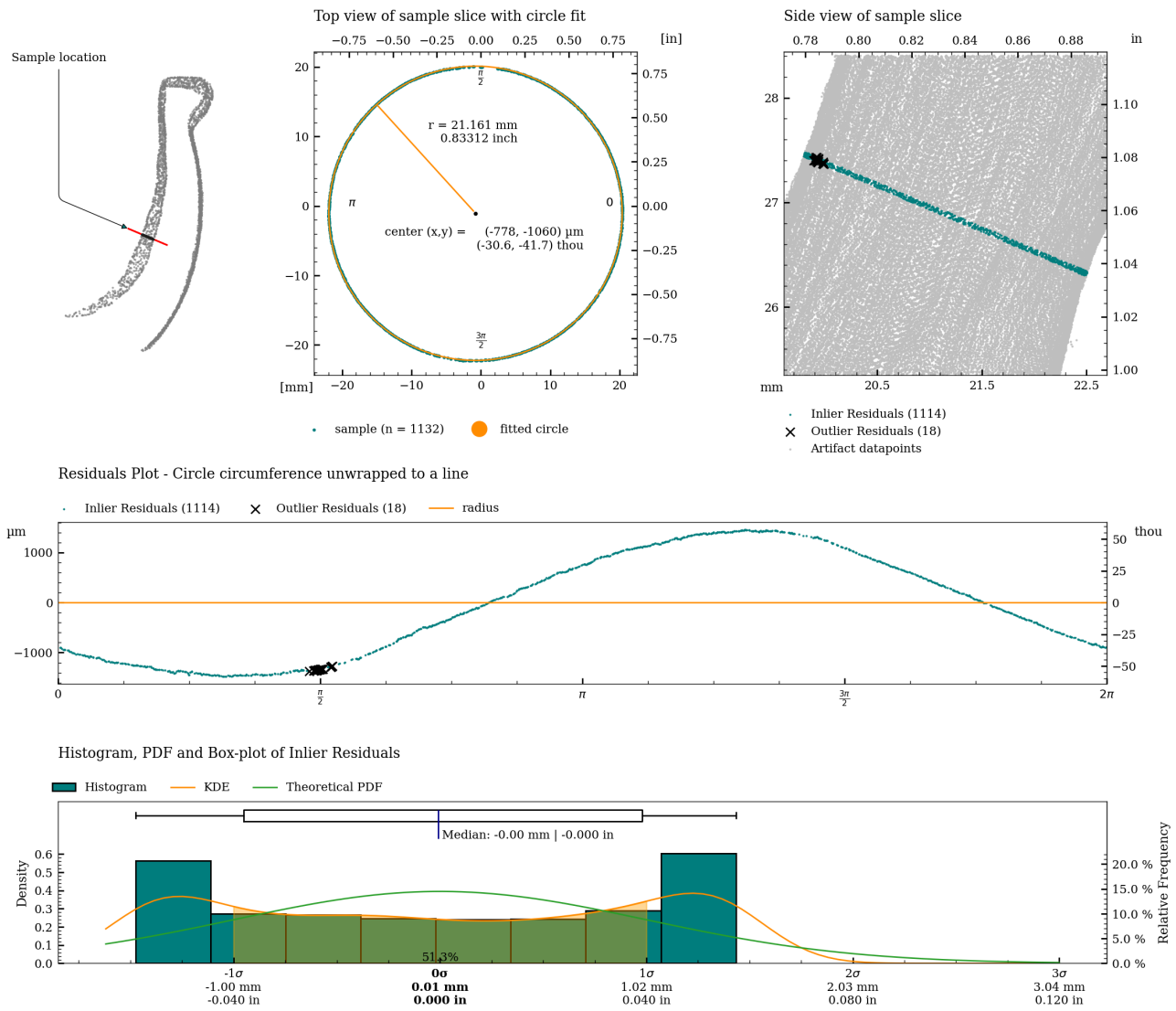


Figure 33: Detailed plot of concentricity measurement for c08.

Concentricity analysis of c09

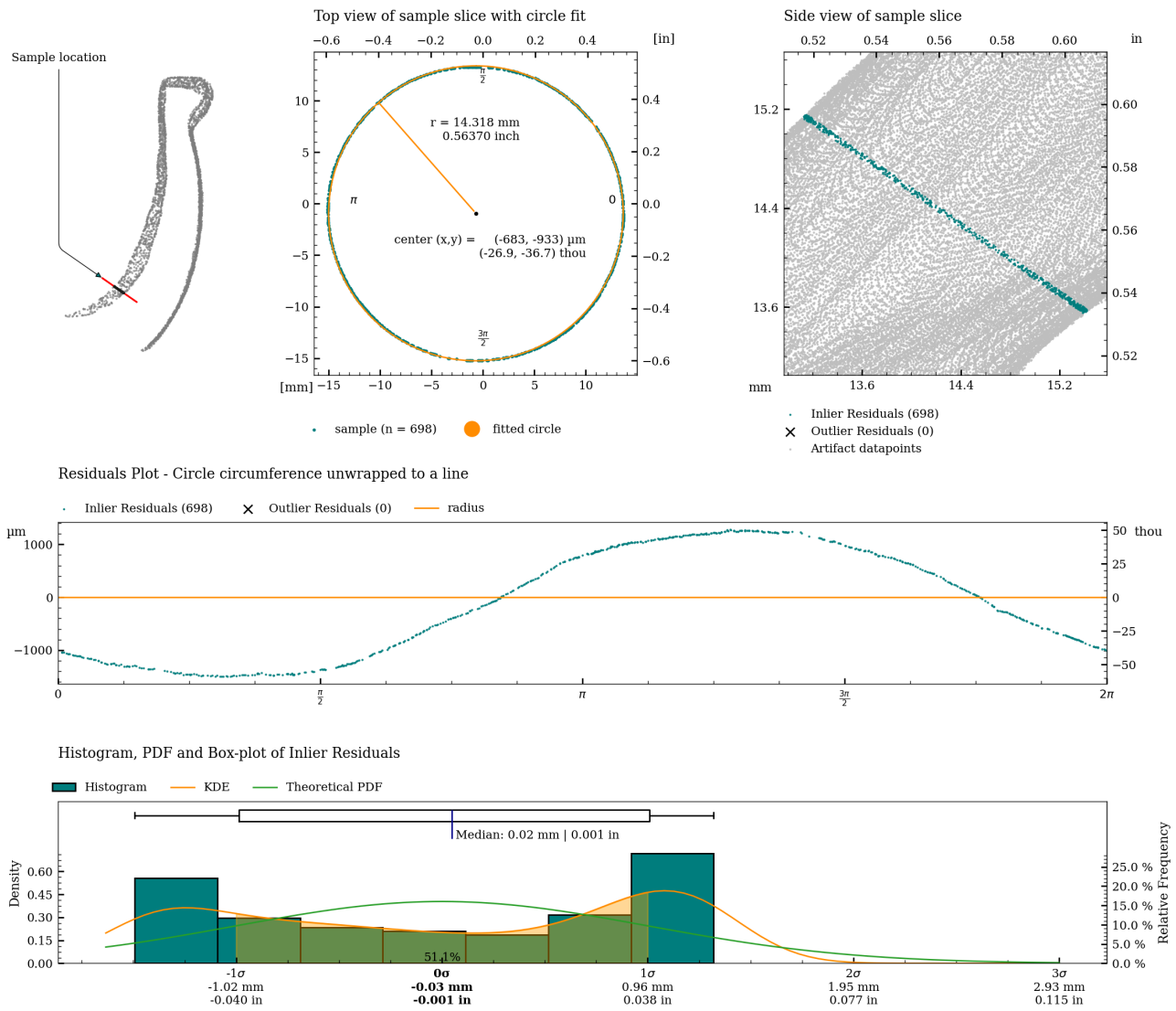


Figure 34: Detailed plot of concentricity measurement for c09.

## Coaxiality

Coaxiality is a measure of the deviation in the central axis of an object. Coaxiality measurements are calculated using RANSAC (Random sample consensus) algorithm for outlier detection of a least squares circle regression on cross-sections of the vessel (excluding potential handles) to estimate the best fit circle centers for each slice of the vessel.

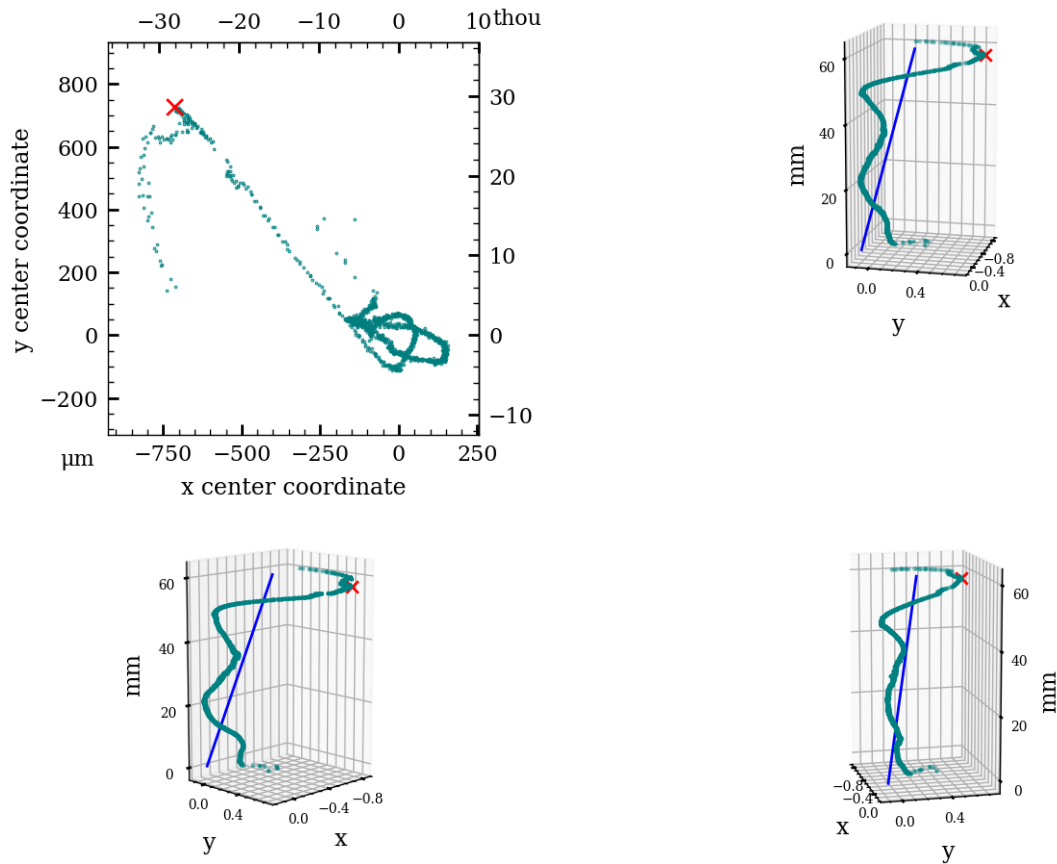
Coaxiality is measured for:

- The exterior surface (excluding handles)
- The interior surface

	Exterior		Interior	
<b>Analyzed Slices</b>		1207		1057
<b>Median sample size</b>		1807		1345
<b>Slice Height</b>	50 $\mu\text{m}$	2.0 thou	50 $\mu\text{m}$	2.0 thou
<b>Statistics with Z-axis as Reference</b>				
Median Absolute Deviation (MAD)	110 $\mu\text{m}$	4.3 thou	1067 $\mu\text{m}$	42.0 thou
Standard Deviation (SD)	264 $\mu\text{m}$	10.4 thou	369 $\mu\text{m}$	14.5 thou
Root Mean Square Deviation (RMSD)	334 $\mu\text{m}$	13.1 thou	1088 $\mu\text{m}$	42.8 thou
<b>Statistics with Best Fit Central Axis as Reference</b>				
Best fit Central Axis Equation (in metric coordinate system with unit [mm])	$x = 0.114 + t \cdot 0.00700$		$x = -1.166 + t \cdot 0.01615$	
	$y = -0.090 + t \cdot 0.00548$		$y = -1.402 + t \cdot 0.01380$	
	$z = 0.000 + t \cdot 0.99996$		$z = 0.000 + t \cdot 0.99977$	
Axis tilt		0.403°		-0.938°
Median Absolute Deviation (MAD)	196 $\mu\text{m}$	7.7 thou	151 $\mu\text{m}$	5.9 thou
Standard Deviation (SD)	145 $\mu\text{m}$	5.7 thou	217 $\mu\text{m}$	8.5 thou
Root Mean Square Deviation (RMSD)	267 $\mu\text{m}$	10.5 thou	306 $\mu\text{m}$	12.0 thou

Table 4: Coaxiality analysis of vessel MV006.

## Coaxiality plots, exterior surface



## Coaxiality residuals from fitted axis, exterior surface

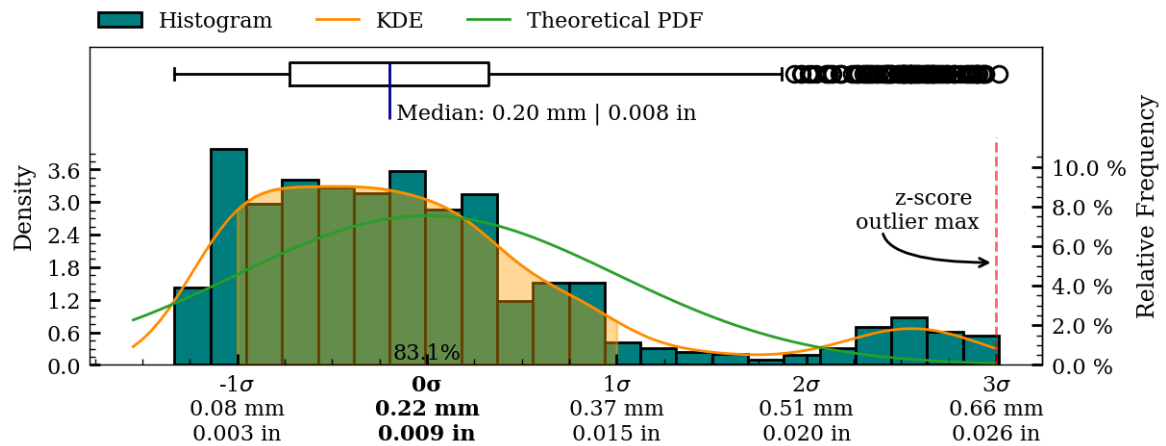
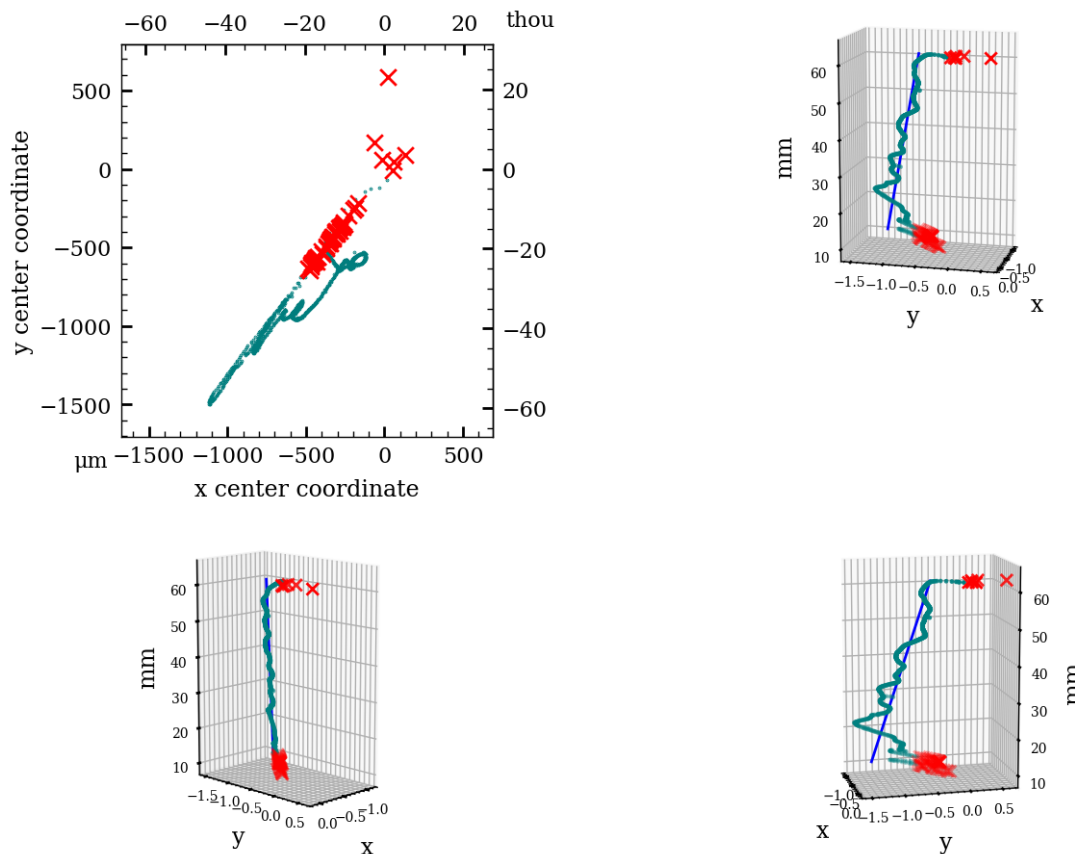


Figure 35: Coaxiality residual plots of exterior surface, MV006.

Coaxiality plots, interior surface



Coaxiality residuals from fitted axis, interior surface

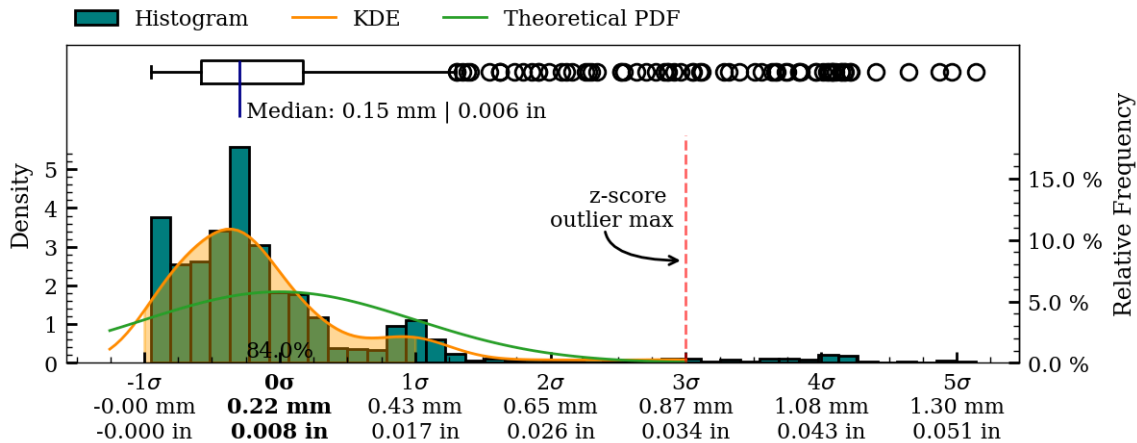


Figure 36: Coaxiality residual plots of interior surface, MV006.

## Surface Variability

To illustrate the overall surface deviations of the object, a surface variability heatmap has been created. This heatmap provides an accessible overview of the topography of the manufacturing precision and surface structure of the object.

The surface variability measurements are created by fitting a number of higher-order polynomials to the two-dimensional folded profile of the scan data. This process creates an idealized mathematical representation of actual surface curvature of object, and as such provides a continuous model representation of the actual object. It is important to note that only such a non-discretized representation is sufficient to avoid introducing inconsistently varying errors in the mapping of the final surface deviation results, that the rendered heatmaps are based on.

To produce the final surface variability map, the distance from each scanned vertex to the fitted polynomial is calculated and used as the mapping function input, for applying colours to the surface of the object.

It is important to note that this variability map does not describe deviations from the original *intended* shape of the artifact (if any), as this shape (the *intended design*, so to speak) will have been lost to time. It does however provide a very informative visualization of the texture and structure of the surface and very importantly, *does* highlight potential manufacturing-relevant patterns in the surface texture (if present). Such patterns are, as an example, clearly evident on the interior surface of artifact PV001.

Exterior surface

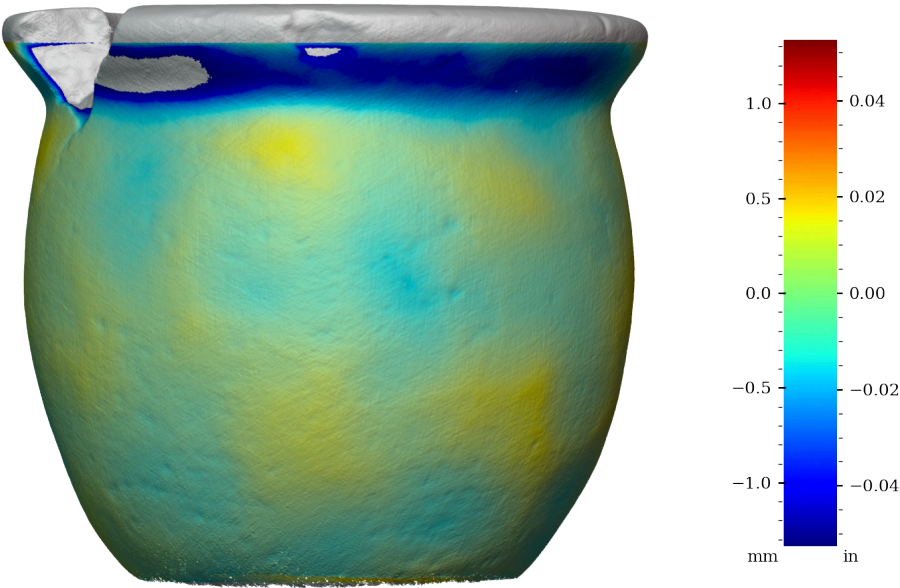


Figure 37: Surface variability heatmap of MV006, front view

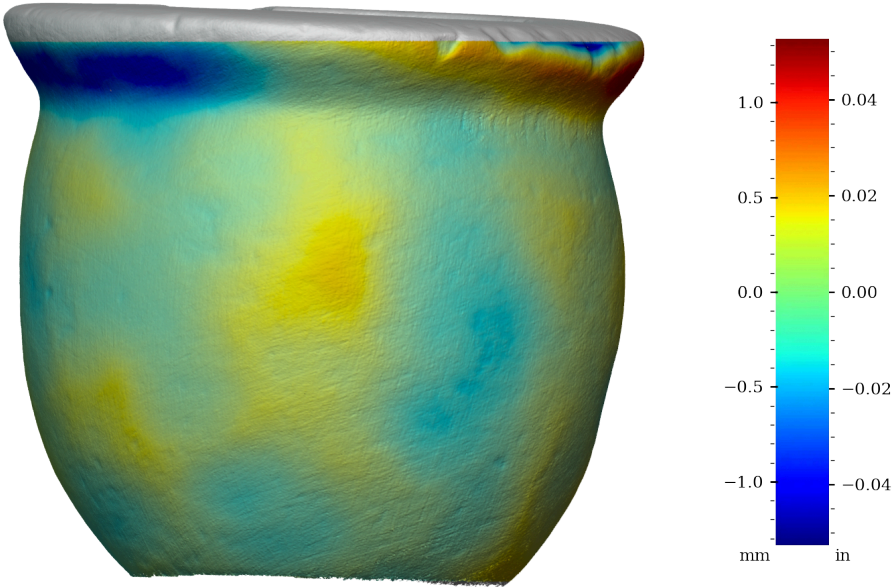


Figure 38: Surface variability heatmap of MV006, rotated 90°

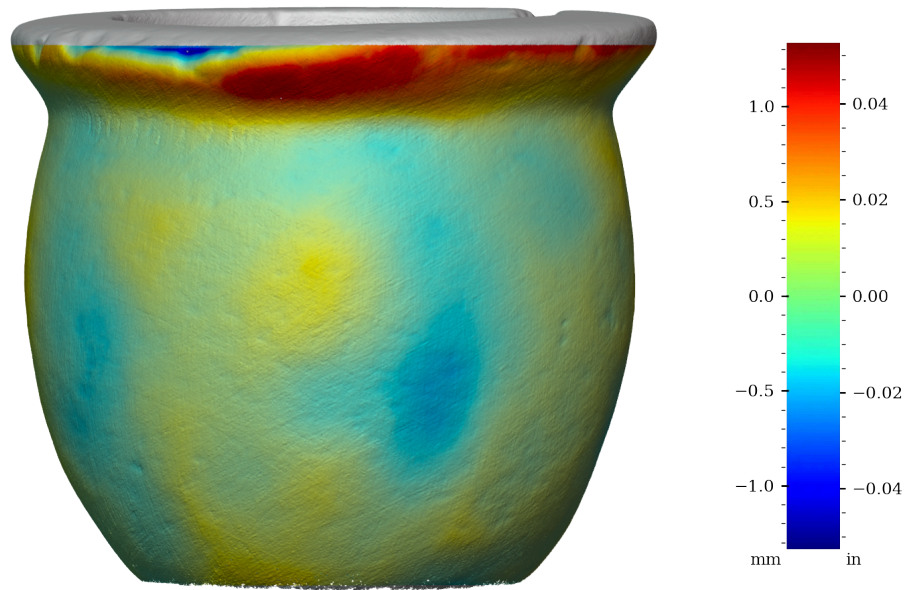


Figure 39: Surface variability heatmap of MV006, rotated 180°

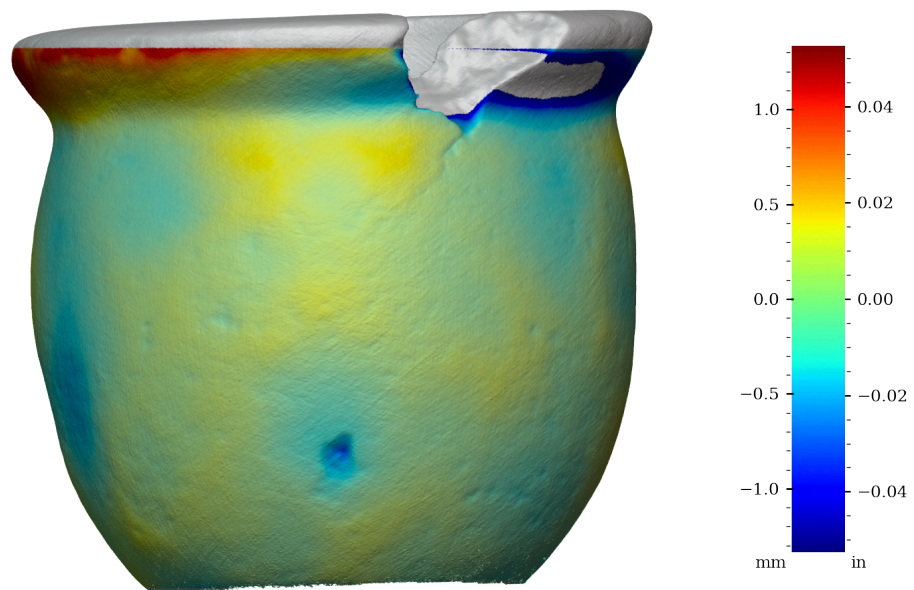


Figure 40: Surface variability heatmap of MV006, rotated 270°

Interior surface

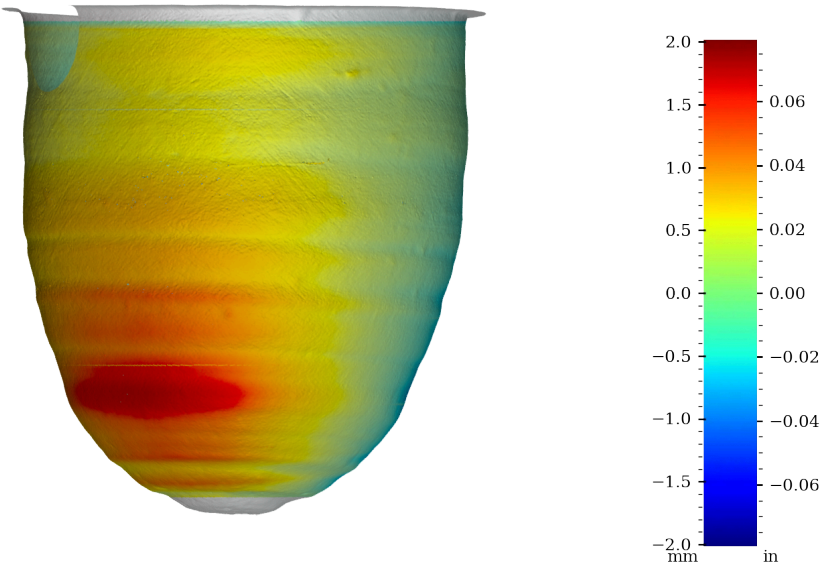


Figure 41: Surface variability heatmap of MV006, front view

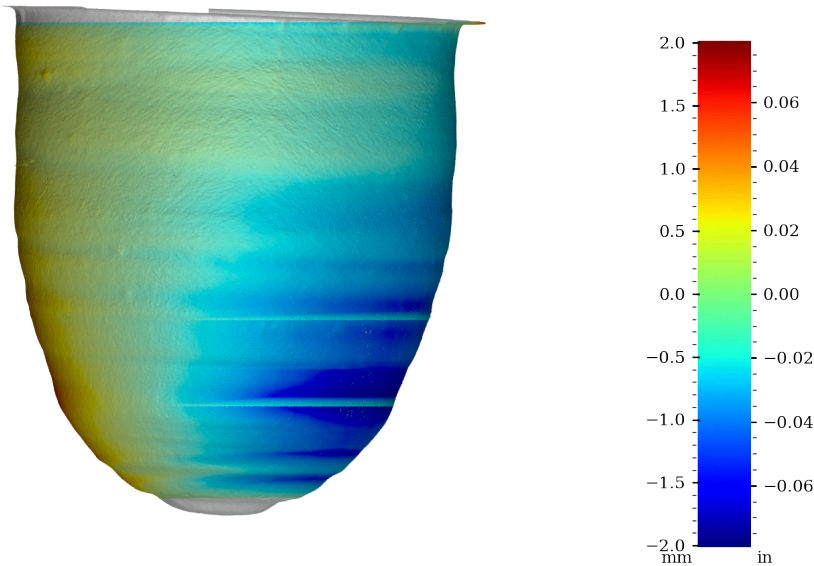


Figure 42: Surface variability heatmap of MV006, rotated 90°

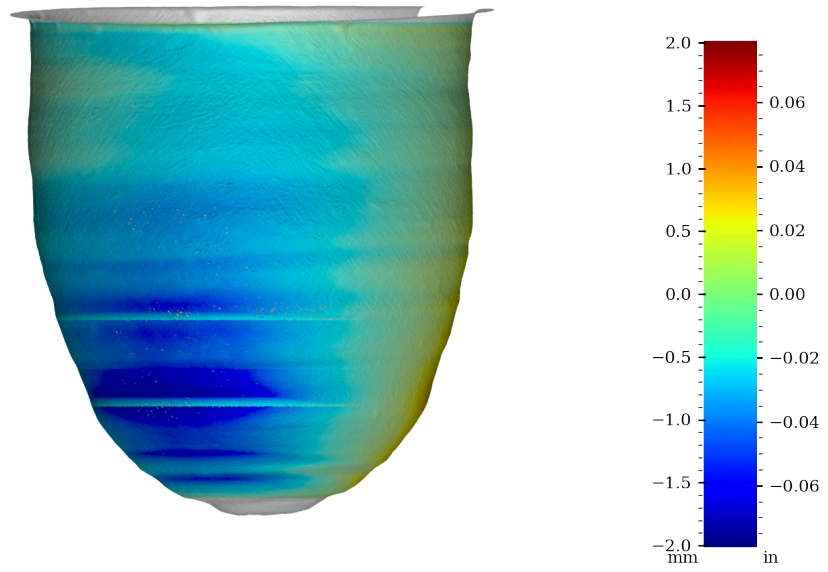


Figure 43: Surface variability heatmap of MV006, rotated 180°

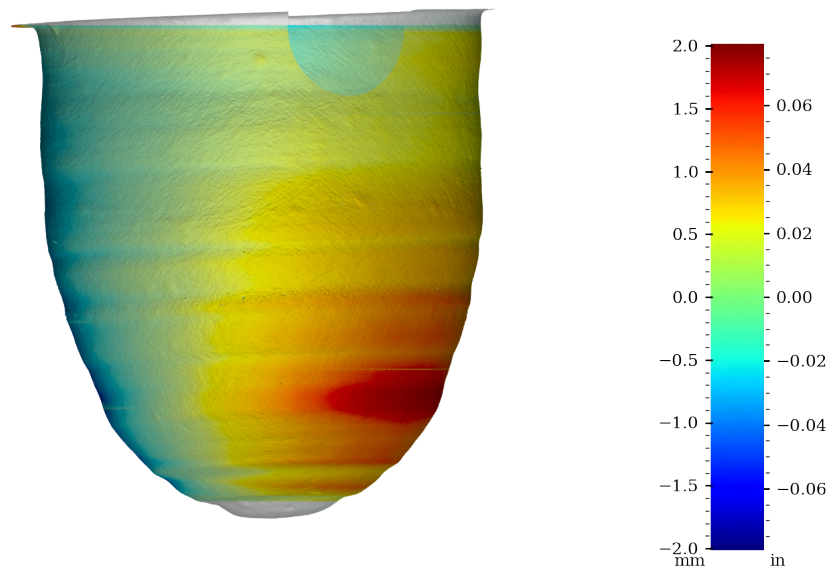


Figure 44: Surface variability heatmap of MV006, rotated 270°

## Surface variability statistics

Area	MSD	RMSD	SD	Mean AD	Median AD	Range	Min	Max	Sample size
	mm <sup>2</sup>	mm	mm	mm	mm	mm	mm	mm	
Exterior	0.1113	0.334	0.334	0.149	0.223	2.905	-1.594	1.311	2333160
Interior	0.6771	0.823	0.823	0.623	0.690	3.994	-2.012	1.982	1460933
	in <sup>2</sup>	in	in	in	in	in	in	in	
Exterior	0.000173	0.0131	0.0131	0.0059	0.0088	0.1144	-0.0628	0.0516	2333160
Interior	0.001050	0.0324	0.0324	0.0245	0.0272	0.1572	-0.0792	0.0780	1460933

Table 5: Surface variability statistics, MV006

Table 5 shows the statistics of the distance from the scan vertices to the best fit object model. These statistics are briefly explained below.

*Mean Squared Deviation* (MSD), also known as Mean Squared Error (MSE).

$$\text{MSD} = \frac{\sum_{i=1}^n (y_i - \hat{y})^2}{n}$$

The MSD metric shows the the average squared difference between the scanned points and the fitted composite polynomial model (a value of 0 would be a perfect match). This metric emphasizes imperfections in the surface of the artifact. Outliers will negatively influence this metric, raising the value of the MSE.

*Root Mean Squared Deviation* (RMSD), also known as Root Mean Squared Error (RMSE).

$$\text{RMSD} = \sqrt{\frac{\sum_{i=1}^n (y_i - \hat{y})^2}{n}}$$

Measures the dispersion of the measured surface variability  $y_i$  around a model predictor ( $\hat{y}$ ). By obtaining the root of the MSD, the exponent will be removed from the measurement, enabling comparisons with other statistics of the same unit and making it more accessible to those familiar with the RMSD metric. This measure is used to assess the fit of a regression model to a dataset, in this case our best fit composite polynomial model. The lower the RMSD metric, the better the fit.

*Standard Deviation* (SD)

$$s = \sqrt{\frac{\sum_{i=1}^n (y_i - \bar{y})^2}{n - 1}}$$

Measures the dispersion of the measured surface variability  $y_i$  around the mean ( $\bar{y}$ ). If the residuals are normally distributed around the mean ( $\bar{y} \approx 0$ ), the SD will be equal to the RMSD. See Figure 45 and Figure 46

*Mean Absolute Deviation* (MeanAD)

$$\text{MeanAD} = \frac{\sum_{i=1}^n |y_i - \bar{y}|}{n}$$

This metric is similar to the SD, but the difference between the residuals and the mean is *not* squared. Instead of indicating the spread of the data, we look at the average distance between each data point and the mean. The Mean Absolute Deviation is affected less by outliers than the Standard Deviation.

*Median Absolute Deviation* (MedianAD)

$$\text{MedianAD} = \text{median}(|y_i - \text{median}(y)|)$$

The Median Absolute Deviation is measure of the dispersion of the data around the median.

*Range*

$$\max(y_i) - \min(y_i)$$

Range is a measure of the total spread of the residuals

## Histogram, KDE and Box-plot of measured surface variability - exterior surface

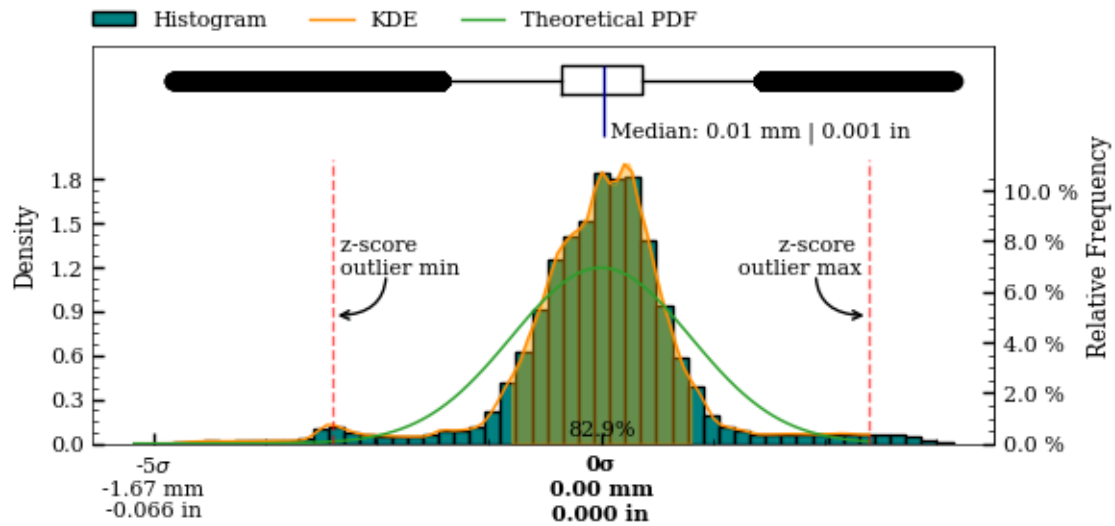


Figure 45: Exterior surface variability boxplot, kds and histogram.

## Histogram, KDE and Box-plot of measured surface variability - interior surface

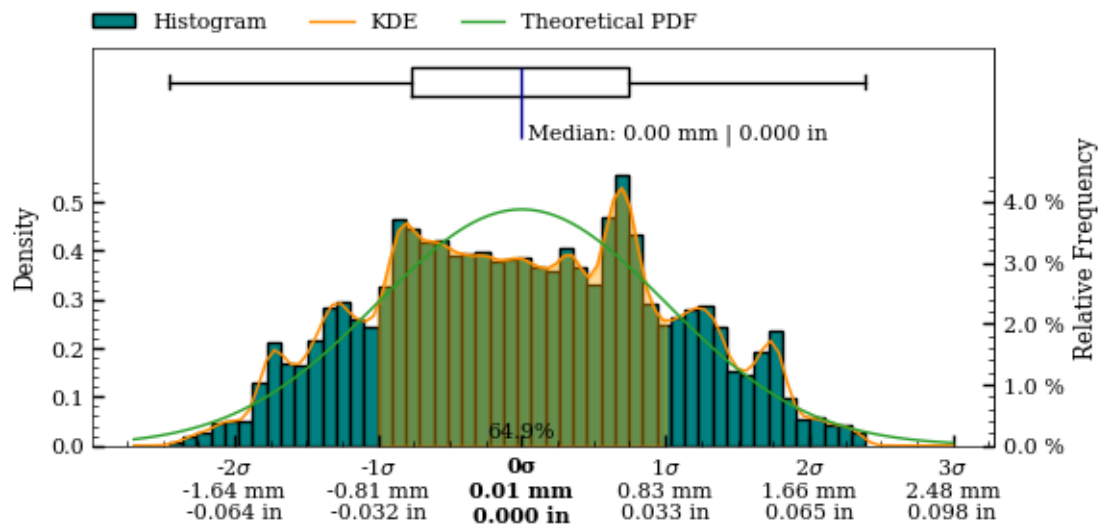


Figure 46: Interior surface variability boxplot, kds and histogram.

## Precision Score Of The Artifact

To enable valid comparison of the manufacturing precision of different artifacts, a metric that robustly quantifies the overall precision of the object is required. The considerations for such a metric will be explored in this section.

Based on these considerations, a *Precision Score* metric will be defined.

For an object to be described as having been manufactured with high precision, several qualities must be present *concurrently*, and throughout the *entire* geometry of the final object. A given object may exhibit high levels of one or more *components* of precision, but be lacking in others. For example:

- An object may present high levels of coaxiality, but lack circularity.
- An object may exhibit good circularity, but show imperfections in the surface structure.
- An object may be smoothed to perfection *without* any circularity or coaxiality.
- An object may exhibit high levels of all of the above metrics in *some* areas, but not in others.

Therefore, a precision score metric **must** account for *all* aspects of the individual, underlying precision metrics (circularity, concentricity, coaxiality and surface variability) throughout the *entire* surface area of the object.

The composite high order polynomial model, used to generate the surface variability map (described in Surface Variability, p. 39) is the best continuous mathematical representation of the object available to us (lacking any original design plans, as would normally be available in metrological analysis). This idealized model encompasses all of the above component metrics.

In the creation of the model, all scan data-points are taken into account (excluding areas with extensive damage), making it the best possible idealized representation we can achieve. When this model has been accurately created, the deviation between the model and the scanned data-points can be calculated over the non-discretized polynomials, *without* the need for an “original” CAD model (and importantly, unless such a CAD model *actually* corresponded to the original design intent, it would be an insufficient comparison basis).

Within the context of defining a valid, overall precision metric, this approach satisfies the incorporation of all of the necessary metrics:

- **Circularity:** Because the reconstructed polynomial model is revolved around the Z-plane, the idealized representation is perfectly circular, and thus incorporates the circularity component.
- **Concentricity and coaxiality:** Because the Z-axis (datum axis) is the center axis of the model, it incorporates the concentricity and coaxiality components.
- **Surface variability:** Because the model is continuous and non-discretized, it can be used accurately for all points of the scan data, and incorporates the surface variability component.

The level of precision ultimately achieved in a physical object does not share a linear relationship with its manufacturing requirements. Since continuously higher levels of final precision becomes progressively harder to achieve, an overall precision metric must take this relationship into account.

A robust statistical metric that satisfies this requirement is the *Mean Squared Deviation* (MSD or MSE). Here specifically, we can utilize the mean square of the deviations between the model ( $\hat{y}$ ) and the data-points ( $y_i$ ).

Combining all of the above considerations, we can express a well-defined *Precision Score* metric, that provides an immediately accessible way to understand the overall precision of an object, while being statistically valid. Since the Mean Squared Deviation tends towards zero as the overall precision increases, the inverse of the Mean Squared Deviation is taken to obtain a precision score metric that increases as precision increases<sup>12</sup>:

$$\text{Precision Score} = \frac{n}{\sum_{i=1}^n (y_i - \hat{y})^2}$$

---


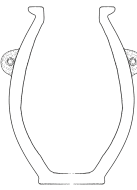

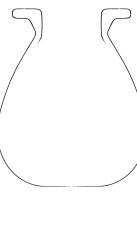



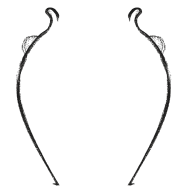


<sup>12</sup>The precision score unit is  $\frac{1}{\text{mm}^2}$

A precision score will be calculated separately for:

- The exterior surface
- The interior surface
- The full surface

As most scans do not include sufficient scan data for the interior surface, the exterior surface will be used for calculating the precision score in most cases. In the rare case that the scan data is more complete for the *interior* surface, this will be used instead.

Table 6 shows the precision score of this artifact (MV006), compared to the two most precise, and the two least precise vessels currently analyzed.

Artifact		Material	Precision Score	Link to Report
		PV001 Red Granite	<b>1905</b>  Full: 980 Exterior: 1905 Interior: 705	Report Publication
		PV006 Dark grey granite	<b>621</b>  Full: 521 Exterior: 621 Interior: 152	Report Publication
		MV006 Basalt	<b>9</b>  Full: 3 Exterior: 9 Interior: 1.48	Report Publication
		MV001 Pottery	<b>1.93</b>  Full: 1.92 Exterior: 1.93 Interior: 1.85	Report Publication
		MV010 Calcite (Egyptian Al-abaster)	<b>1.12</b>  Full: 0.64 Exterior: 1.12 Interior: 0.20	Report Publication (Draft - Awaiting publication)

# Analysis Roadmap

While the current iteration of this work already provides valuable results, continued future additions and improvements will enhance their utility further. This section details planned iterative updates and improvements, to both the reports themselves, and to the underlying methodology and software they are created with.

## Alignment Section

- Detailed exploration of different circle regression algorithms
- If handles are present on the vessel, exploring alignment of the vessels so the handle positions match each other
- Add optimization of the perpendicular surface deviation, with the best results of the coaxial alignment
- Align by minimizing circularity results (of rotated sample slice, to compensate for sample height distortions)

## Measurements of Precision

- Section detailing how measurements perpendicular to the surface curvature are obtained
- Detailed surface area analysis, exploring the residual patterns throughout subsequent sample slices of the artifact surface
- Wall thickness deviation color map
- Robust outlier identification on circularity, to better handle analysis of damaged areas of the artifacts in addition to removal of interior crystalline structure points present in CT scans
- Layout updates to the charts and tables

## Visibility of Outliers and Damaged Sections

- Identification and marking of damaged parts
- Visualization of outliers on the artifact surface

## Exploration of Mathematical Primitives

- Analysis of selected curvatures and flat surfaces on the vessel in both the horizontal and vertical planes
  - Circles
  - Parabolas
  - Ellipsoids
  - Hyperbolas
  - Cones
- Implementation of robust regressions models suitable for this domain, based on RANSAC.

## Metrics on Primary Features

- Measurements of features in the horizontal plane
- Measurements of features in the vertical plane
- Measurements of angles
- Measurements of volume

## Exploration of Potential Design Ratios

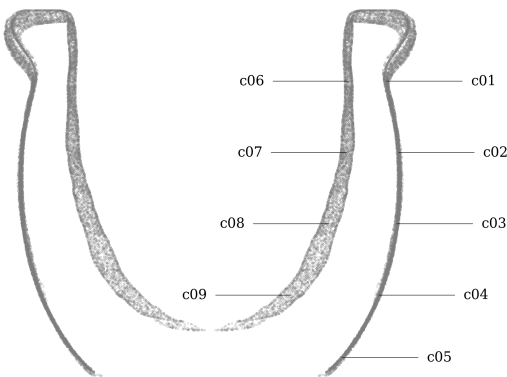
- $\pi$ ,  $\varphi$ ,  $e$ , 1, 2, 3, 4 etc.

## Raw Dataset Attachments

- Including all measurement and sample coordinates as CSV-files embedded in the report
- Including an STL file of the aligned object alongside the report, for easier external replication and validation of the research results

# Appendix A - Comparison Of Circularity Measurements (Z-plane vs. surface-perpendicular)

## Comparison of circularity samples



## Samples perpendicular to the surface curvature

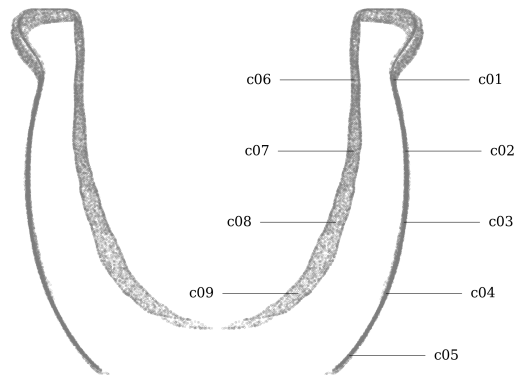
Tag	Area	Measured deviation <sup>8</sup>	Residuals				Sample size	Slice		
			Range	RMSD <sup>9</sup>	MAD <sup>10</sup>	SD		Height	Z coord.	Radius <sup>11</sup>
		mm	mm	mm	mm	mm		mm	mm	mm
c01	exterior	Ø62.863±0.516	1.012	0.275	0.196	0.276	1762	0.050	52.209	31.431
c02	exterior	Ø67.109±0.436	0.812	0.167	0.117	0.167	1960	0.050	39.545	33.555
c03	exterior	Ø66.558±0.503	0.818	0.191	0.132	0.191	2010	0.050	26.881	33.279
c04	exterior	Ø60.183±0.756	1.124	0.187	0.134	0.187	1645	0.050	14.218	30.091
c05	exterior	Ø47.151±0.437	0.714	0.167	0.107	0.167	1108	0.050	3.154	23.576
c06	interior	Ø49.365±0.754	1.411	0.459	0.449	0.460	1491	0.050	52.209	24.683
c07	interior	Ø48.677±1.141	2.165	0.763	0.788	0.763	1451	0.050	39.545	24.339
c08	interior	Ø42.346±1.493	2.937	1.016	0.992	1.017	1132	0.050	26.881	21.173
c09	interior	Ø28.936±1.626	2.778	0.999	0.928	0.988	698	0.050	14.218	14.468

Table 7: Detailed circularity measurements at selected samples in z-plane, vessel MV006.

## Samples in the Z-plane

Tag	Area	Measured deviation <sup>8</sup>	Residuals				Sample size	Slice		
			Range	RMSD <sup>9</sup>	MAD <sup>10</sup>	SD		Height	Z coord.	Radius <sup>11</sup>
		mm	mm	mm	mm	mm		mm	mm	mm
c01	exterior	Ø62.972±0.570	1.017	0.283	0.208	0.277	1779	0.050	52.209	31.486
c02	exterior	Ø67.096±0.454	0.823	0.171	0.116	0.171	1973	0.050	39.545	33.548
c03	exterior	Ø66.651±0.559	0.828	0.194	0.100	0.190	1992	0.050	26.881	33.325
c04	exterior	Ø60.251±0.759	1.126	0.198	0.127	0.195	1921	0.050	14.218	30.125
c05	exterior	Ø47.106±0.587	1.007	0.216	0.129	0.214	1869	0.050	3.154	23.553
c06	interior	Ø49.423±0.784	1.408	0.468	0.460	0.466	1528	0.050	52.209	24.711
c07	interior	Ø48.754±1.191	2.209	0.771	0.792	0.770	1438	0.050	39.545	24.377
c08	interior	Ø42.310±1.597	3.173	1.101	1.105	1.101	1324	0.050	26.881	21.155
c09	interior	Ø28.944±2.248	4.216	1.458	1.472	1.459	1177	0.050	14.218	14.472

Table 8: Detailed circularity measurements at selected samples perpendicular to vessel curvature, vessel MV006.



### Samples perpendicular to the surface curvature

Tag	Area	Measured deviation <sup>8</sup>	Residuals				Sample size	Slice		
			Range	RMSD <sup>9</sup>	MAD <sup>10</sup>	SD		Height	Z coord.	Radius <sup>11</sup>
		in	in	in	in	in		in	in	in
c01	exterior	Ø2.4749±0.0203	0.0398	0.0108	0.0077	0.0108	1762	0.0020	2.0555	1.2375
c02	exterior	Ø2.6421±0.0172	0.0320	0.0066	0.0046	0.0066	1960	0.0020	1.5569	1.3210
c03	exterior	Ø2.6204±0.0198	0.0322	0.0075	0.0052	0.0075	2010	0.0020	1.0583	1.3102
c04	exterior	Ø2.3694±0.0298	0.0442	0.0073	0.0053	0.0073	1645	0.0020	0.5598	1.1847
c05	exterior	Ø1.8564±0.0172	0.0281	0.0066	0.0042	0.0066	1108	0.0020	0.1242	0.9282
c06	interior	Ø1.9435±0.0297	0.0555	0.0181	0.0177	0.0181	1491	0.0020	2.0555	0.9718
c07	interior	Ø1.9164±0.0449	0.0853	0.0300	0.0310	0.0300	1451	0.0020	1.5569	0.9582
c08	interior	Ø1.6672±0.0588	0.1156	0.0400	0.0390	0.0400	1132	0.0020	1.0583	0.8336
c09	interior	Ø1.1392±0.0640	0.1094	0.0393	0.0365	0.0389	698	0.0020	0.5598	0.5696

Table 9: Detailed circularity measurements at selected samples in z-plane, vessel MV006.

### Samples in the Z-plane

Tag	Area	Measured deviation <sup>8</sup>	Residuals				Sample size	Slice		
			Range	RMSD <sup>9</sup>	MAD <sup>10</sup>	SD		Height	Z coord.	Radius <sup>11</sup>
		in	in	in	in	in		in	in	in
c01	exterior	Ø2.4792±0.0224	0.0400	0.0111	0.0082	0.0109	1779	0.0020	2.0555	1.2396
c02	exterior	Ø2.6416±0.0179	0.0324	0.0067	0.0046	0.0067	1973	0.0020	1.5569	1.3208
c03	exterior	Ø2.6240±0.0220	0.0326	0.0076	0.0039	0.0075	1992	0.0020	1.0583	1.3120
c04	exterior	Ø2.3721±0.0299	0.0443	0.0078	0.0050	0.0077	1921	0.0020	0.5598	1.1860
c05	exterior	Ø1.8546±0.0231	0.0397	0.0085	0.0051	0.0084	1869	0.0020	0.1242	0.9273
c06	interior	Ø1.9458±0.0309	0.0554	0.0184	0.0181	0.0184	1528	0.0020	2.0555	0.9729
c07	interior	Ø1.9195±0.0469	0.0870	0.0303	0.0312	0.0303	1438	0.0020	1.5569	0.9597
c08	interior	Ø1.6657±0.0629	0.1249	0.0434	0.0435	0.0434	1324	0.0020	1.0583	0.8329
c09	interior	Ø1.1395±0.0885	0.1660	0.0574	0.0580	0.0574	1177	0.0020	0.5598	0.5698

Table 10: Detailed circularity measurements at selected samples perpendicular to vessel curvature, vessel MV006.

# Comparison of circularity on the full vessel surface

Metric

## Samples perpendicular to the surface curvature

Area	Range			Standard Deviation			Medan Absolute Deviation			Slices	Slice height
	Median	Min.	Max.	Median	Min.	Max.	Median	Min.	Max.		
	mm	mm	mm	mm	mm	mm	mm	mm	mm		mm
Exterior	0.860	0.567	3.058	0.195	0.143	0.807	0.012	0.070	0.830	1207	0.050
Interior	2.016	0.559	3.597	0.640	0.148	1.101	0.179	0.085	1.104	1057	0.050

Table 11: Detailed circularity measurements at selected samples in z-plane, vessel MV006.

## Samples in the z-plane

Area	Range			Standard Deviation			Medan Absolute Deviation			Slices	Slice height
	Median	Min.	Max.	Median	Min.	Max.	Median	Min.	Max.		
	mm	mm	mm	mm	mm	mm	mm	mm	mm		mm
Exterior	0.911	0.629	3.570	0.205	0.158	1.065	0.016	0.085	0.967	1205	0.050
Interior	2.469	1.098	4.478	0.841	0.314	1.572	0.358	0.207	1.614	1062	0.050

Table 12: Detailed circularity measurements at selected samples perpendicular to vessel curvature, vessel MV006.

Imperial

## Samples perpendicular to the surface curvature

Area	Range			Standard Deviation			Medan Absolute Deviation			Slices	Slice height
	Median	Min.	Max.	Median	Min.	Max.	Median	Min.	Max.		
	in	in	in	in	in	in	in	in	in		in
Exterior	0.860	0.567	3.058	0.195	0.143	0.807	0.012	0.070	0.830	1207	0.050
Interior	2.016	0.559	3.597	0.640	0.148	1.101	0.179	0.085	1.104	1057	0.050

Table 13: Detailed circularity measurements at selected samples in z-plane, vessel MV006.

## Samples in the z-plane

Area	Range			Standard Deviation			Medan Absolute Deviation			Slices	Slice height
	Median	Min.	Max.	Median	Min.	Max.	Median	Min.	Max.		
	in	in	in	in	in	in	in	in	in		in
Exterior	0.911	0.629	3.570	0.205	0.158	1.065	0.016	0.085	0.967	1205	0.050
Interior	2.469	1.098	4.478	0.841	0.314	1.572	0.358	0.207	1.614	1062	0.050

Table 14: Detailed circularity measurements at selected samples perpendicular to vessel curvature, vessel MV006.

Circularity analysis of exterior samples perpendicular to surface curvature

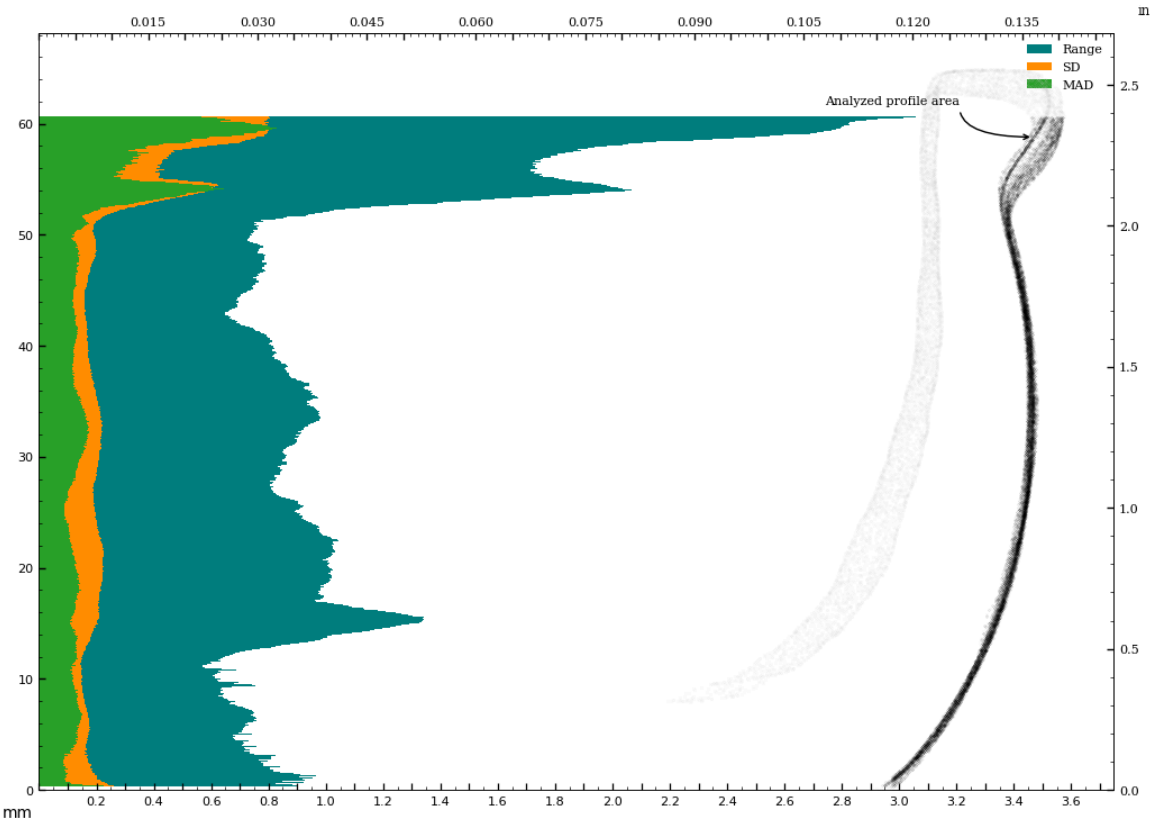


Figure 47: Circularity analysis of exterior samples perpendicular to surface curvature

Circularity analysis of exterior surface - in z-plane

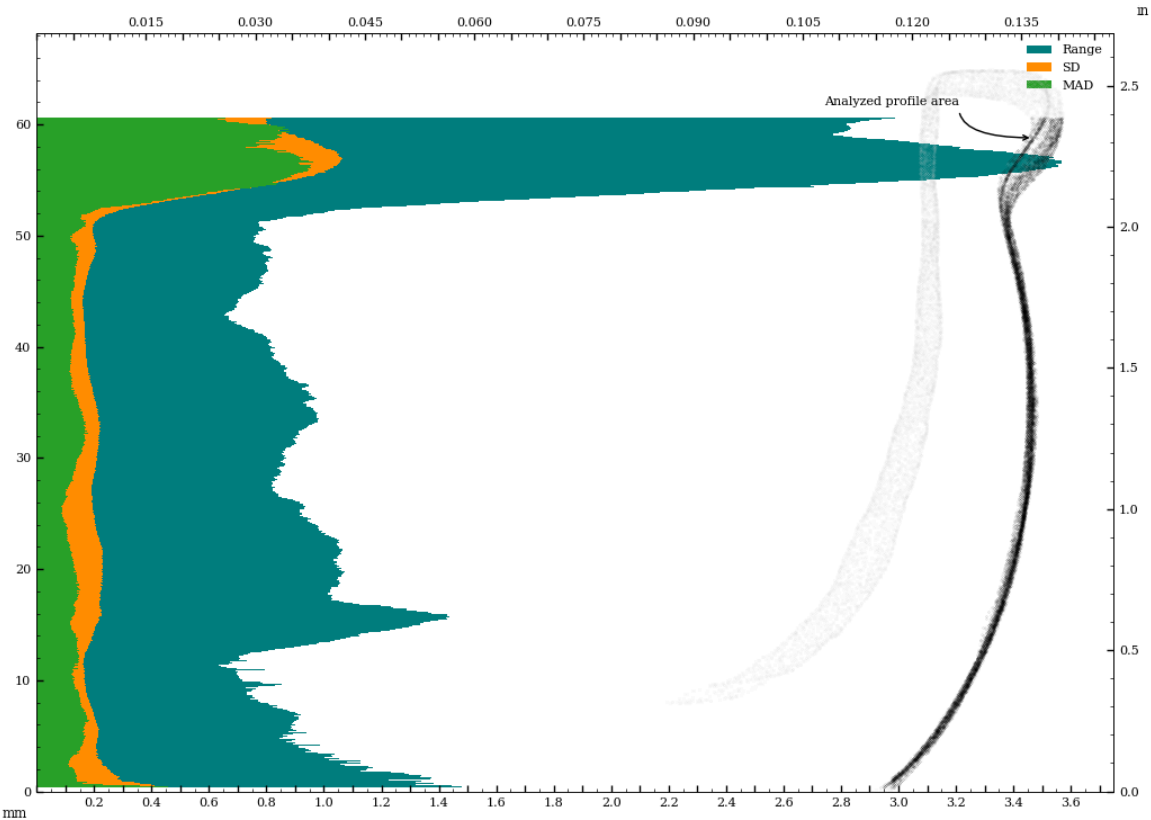


Figure 48: Circularity analysis of exterior surface - in z-plane

Circularity analysis of exterior samples perpendicular to surface curvature

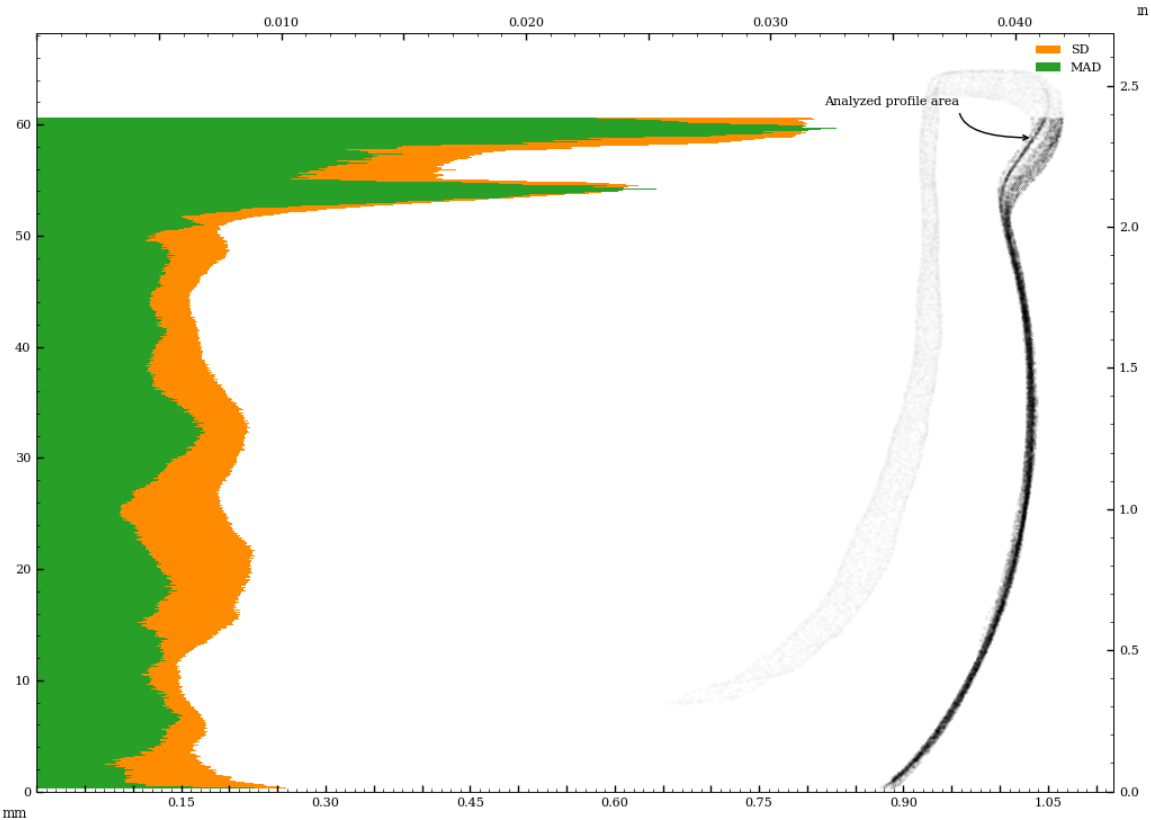


Figure 49: Circularity analysis of exterior samples perpendicular to surface curvature

Circularity analysis of exterior surface - in z-plane

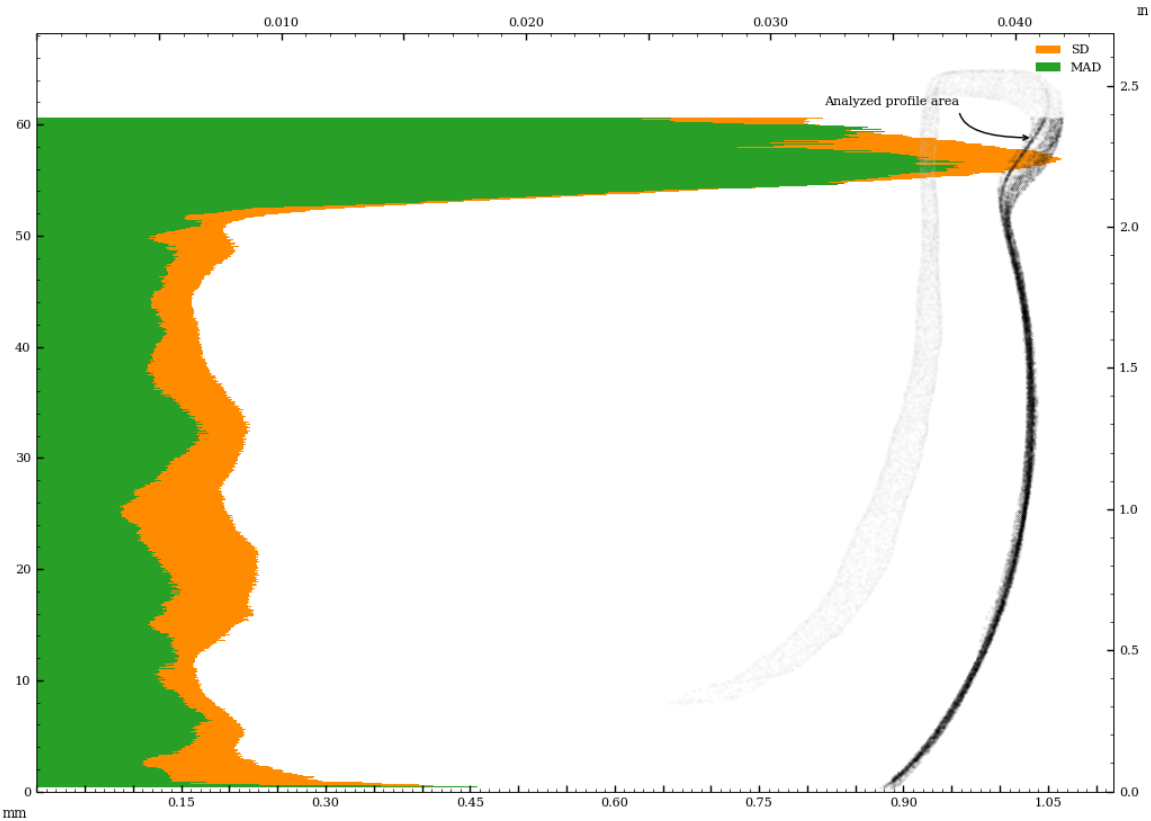


Figure 50: Circularity analysis of exterior surface - in z-plane

Circularity analysis of interior samples perpendicular to surface curvature

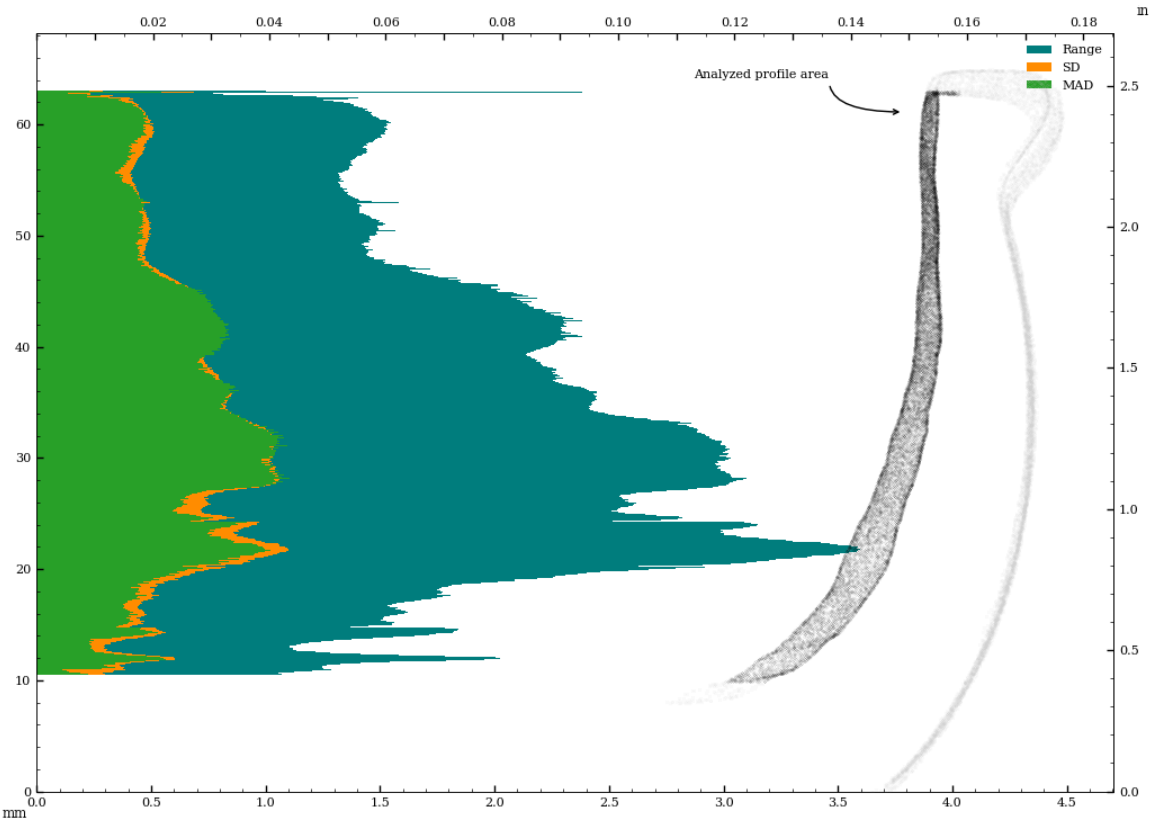


Figure 51: Circularity analysis of interior samples perpendicular to surface curvature

Circularity analysis of interior surface - in z-plane

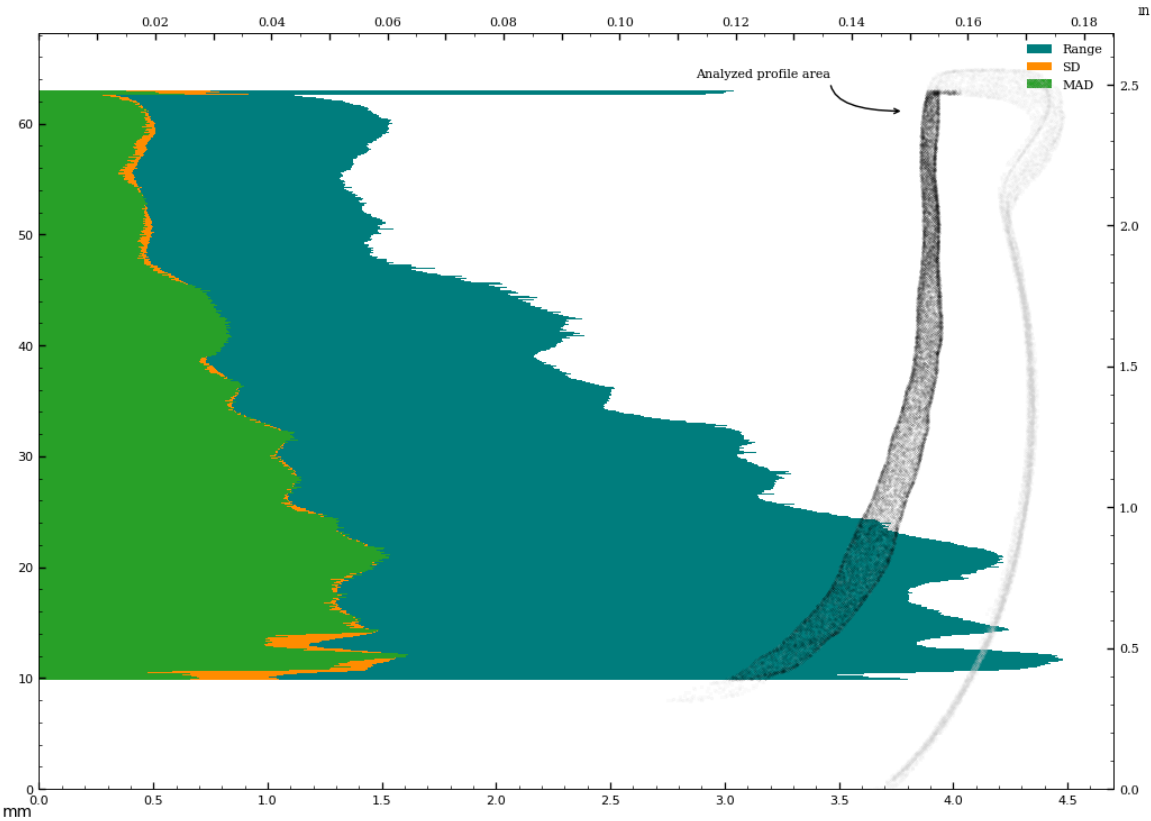


Figure 52: Circularity analysis of interior surface - in z-plane

Circularity analysis of interior samples perpendicular to surface curvature

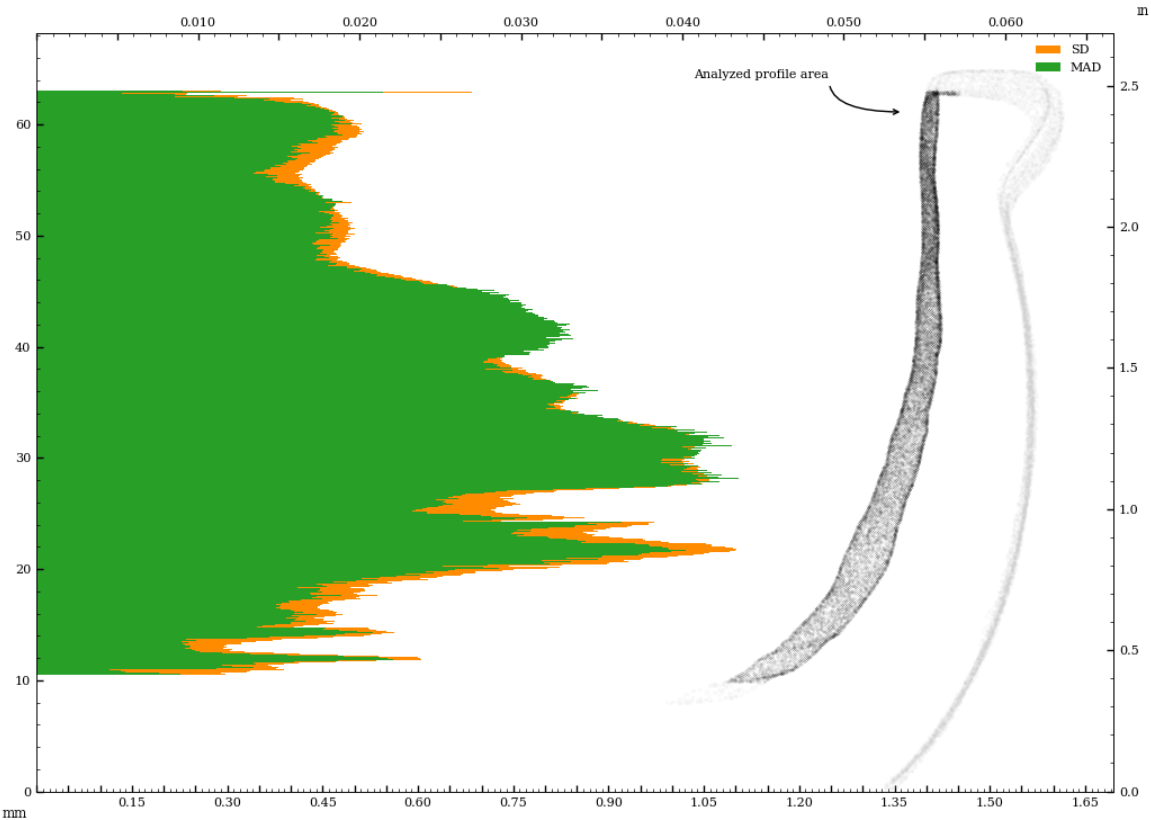


Figure 53: Circularity analysis of interior samples perpendicular to surface curvature

Circularity analysis of interior surface - in z-plane

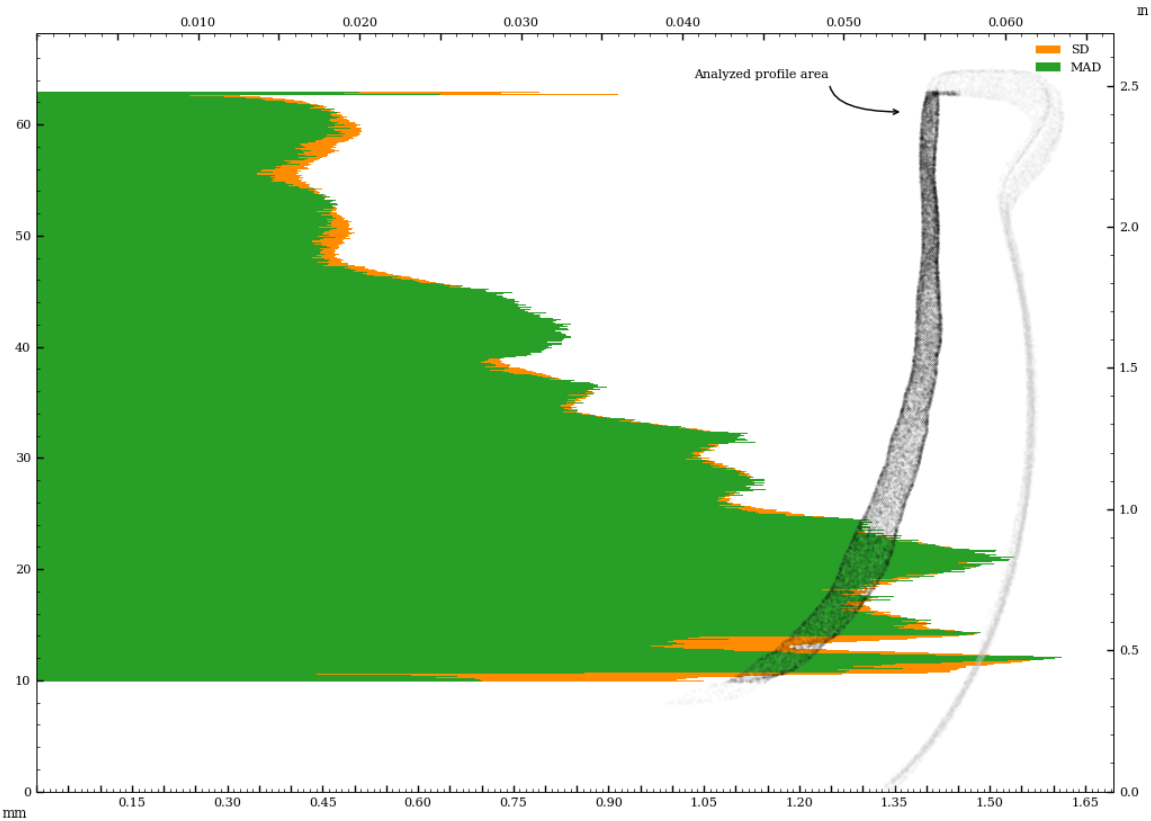


Figure 54: Circularity analysis of interior surface - in z-plane

## Appendix B - Comparison Of Concentricity Measurements (Z-plane vs. surface-perpendicular)

Metric

### Concentricity measurements perpendicular to surface curvature

Tag	Reference	Deviation	Sample size	Circle fit residuals analysis for sample listed in Tag column						
				Range full	Range inliers	SD full	SD inliers	MAD full	MAD inliers	Center (x,y)
		mm		mm	mm	mm	mm	mm	mm	μm
c01	z-axis	0.304	1762	1.012	1.012	0.276	0.276	0.199	0.199	−259, 160
c02	z-axis	0.066	1960	0.812	0.812	0.167	0.167	0.114	0.114	−3, 66
c03	z-axis	0.061	2010	0.818	0.776	0.191	0.175	0.103	0.098	−10, −60
c04	z-axis	0.082	1645	1.124	0.915	0.187	0.172	0.124	0.122	82, 9
c05	z-axis	0.137	1108	0.714	0.714	0.167	0.167	0.099	0.099	−114, 75
c06	z-axis	0.638	1491	1.411	1.411	0.460	0.462	0.455	0.456	−196, −607
c07	z-axis	1.041	1451	2.165	2.165	0.763	0.763	0.785	0.785	−556, −880
c08	z-axis	1.315	1132	2.937	2.937	1.017	1.011	0.992	0.977	−778, −1060
c09	z-axis	1.157	698	2.778	2.778	0.988	0.988	0.970	0.970	−683, −933
c01	c06	0.770	1762	1.012	1.012	0.276	0.276	0.199	0.199	−63, 767
c02	c07	1.095	1960	0.812	0.812	0.167	0.167	0.114	0.114	553, 946
c03	c08	1.261	2010	0.818	0.776	0.191	0.175	0.103	0.098	768, 1000
c04	c09	1.214	1645	1.124	0.915	0.187	0.172	0.124	0.122	765, 942

### Concentricity measurements in z-plane

Tag	Reference	Deviation	Sample size	Circle fit residuals analysis for sample listed in Tag column						
				Range full	Range inliers	SD full	SD inliers	MAD full	MAD inliers	Center (x,y)
		mm		mm	mm	mm	mm	mm	mm	μm
c01	z-axis	0.307	1779	1.225	1.225	0.282	0.282	0.207	0.207	−261, 161
c02	z-axis	0.064	1973	0.948	0.948	0.193	0.193	0.135	0.135	1, 64
c03	z-axis	0.053	1992	0.809	0.809	0.202	0.190	0.140	0.135	−1, −53
c04	z-axis	0.089	1921	1.168	1.021	0.201	0.188	0.131	0.129	87, 17
c05	z-axis	0.233	1869	1.196	1.196	0.242	0.242	0.162	0.162	−187, 138
c06	z-axis	0.642	1528	3.018	3.018	1.047	1.051	1.060	1.071	−197, −611
c07	z-axis	1.073	1438	4.662	4.662	1.666	1.666	1.698	1.698	−577, −904
c08	z-axis	1.549	1324	6.634	6.634	2.339	2.332	2.363	2.338	−918, −1248
c09	z-axis	2.068	1177	8.835	8.835	3.089	3.078	3.044	2.989	−1228, −1664
c01	c06	0.775	1779	1.225	1.225	0.282	0.282	0.207	0.207	−64, 772
c02	c07	1.128	1973	0.948	0.948	0.193	0.193	0.135	0.135	578, 969
c03	c08	1.506	1992	0.809	0.809	0.202	0.190	0.140	0.135	916, 1195
c04	c09	2.135	1921	1.168	1.021	0.201	0.188	0.131	0.129	1316, 1681

# Imperial

## Concentricity measurements perpendicular to surface curvature

Tag	Reference	Deviation	Sample size	Circle fit residuals analysis for sample listed in Tag column						
				Range full	Range inliers	SD full	SD inliers	MAD full	MAD inliers	Center (x,y)
		in		in	in	in	in	in	in	thou
c01	z-axis	0.0120	1762	0.0398	0.0398	0.0108	0.0108	0.0078	0.0078	−10.2, 6.3
c02	z-axis	0.0026	1960	0.0320	0.0320	0.0066	0.0066	0.0045	0.0045	−0.1, 2.6
c03	z-axis	0.0024	2010	0.0322	0.0305	0.0075	0.0069	0.0040	0.0039	−0.4, −2.4
c04	z-axis	0.0032	1645	0.0442	0.0360	0.0073	0.0068	0.0049	0.0048	3.2, 0.4
c05	z-axis	0.0054	1108	0.0281	0.0281	0.0066	0.0066	0.0039	0.0039	−4.5, 2.9
c06	z-axis	0.0251	1491	0.0555	0.0555	0.0181	0.0182	0.0179	0.0180	−7.7, −23.9
c07	z-axis	0.0410	1451	0.0853	0.0853	0.0300	0.0300	0.0309	0.0309	−21.9, −34.6
c08	z-axis	0.0518	1132	0.1156	0.1156	0.0400	0.0398	0.0390	0.0385	−30.6, −41.7
c09	z-axis	0.0455	698	0.1094	0.1094	0.0389	0.0389	0.0382	0.0382	−26.9, −36.7
c01	c06	0.0303	1762	0.0398	0.0398	0.0108	0.0108	0.0078	0.0078	−2.5, 30.2
c02	c07	0.0431	1960	0.0320	0.0320	0.0066	0.0066	0.0045	0.0045	21.8, 37.2
c03	c08	0.0497	2010	0.0322	0.0305	0.0075	0.0069	0.0040	0.0039	30.2, 39.4
c04	c09	0.0478	1645	0.0442	0.0360	0.0073	0.0068	0.0049	0.0048	30.1, 37.1

## Concentricity measurements in z-plane

Tag	Reference	Deviation	Sample size	Circle fit residuals analysis for sample listed in Tag column						
				Range full	Range inliers	SD full	SD inliers	MAD full	MAD inliers	Center (x,y)
		in		in	in	in	in	in	in	thou
c01	z-axis	0.0121	1779	0.0482	0.0482	0.0111	0.0111	0.0082	0.0082	−10.3, 6.3
c02	z-axis	0.0025	1973	0.0373	0.0373	0.0076	0.0076	0.0053	0.0053	0.0, 2.5
c03	z-axis	0.0021	1992	0.0319	0.0319	0.0080	0.0075	0.0055	0.0053	−0.1, −2.1
c04	z-axis	0.0035	1921	0.0460	0.0402	0.0079	0.0074	0.0052	0.0051	3.4, 0.7
c05	z-axis	0.0092	1869	0.0471	0.0471	0.0095	0.0095	0.0064	0.0064	−7.4, 5.4
c06	z-axis	0.0253	1528	0.1188	0.1188	0.0412	0.0414	0.0417	0.0422	−7.8, −24.0
c07	z-axis	0.0422	1438	0.1835	0.1835	0.0656	0.0656	0.0668	0.0668	−22.7, −35.6
c08	z-axis	0.0610	1324	0.2612	0.2612	0.0921	0.0918	0.0930	0.0920	−36.1, −49.1
c09	z-axis	0.0814	1177	0.3478	0.3478	0.1216	0.1212	0.1198	0.1177	−48.4, −65.5
c01	c06	0.0305	1779	0.0482	0.0482	0.0111	0.0111	0.0082	0.0082	−2.5, 30.4
c02	c07	0.0444	1973	0.0373	0.0373	0.0076	0.0076	0.0053	0.0053	22.8, 38.1
c03	c08	0.0593	1992	0.0319	0.0319	0.0080	0.0075	0.0055	0.0053	36.1, 47.0
c04	c09	0.0840	1921	0.0460	0.0402	0.0079	0.0074	0.0052	0.0051	51.8, 66.2